PHI User Manual v3

Nicholas F. Chilton

Contents

License

PHI
Nicholas F. Chilton
email: nfchilton@gmail.com

This document is part of PHI.

We request that any results obtained through the use of PHI are accompanied by the following reference:

N. F. Chilton, R. P. Anderson, L. D. Turner, A. Soncini and K. S. Murray,
J. Comput. Chem., 2013, **34**, 1164 – 1175.

Acknowledgements

The author wishes to acknowledge advice, assistance and contributions from the following people:

Prof. Keith Murray[a]
Prof. Stuart Batten[a]
Prof. Richard Winpenny[b]
Prof. Eric McInnes[b]
Prof. David Collison[b]
Prof. Fernande Grandjean[c]
Assoc. Prof. Alessandro Soncini[e]
Dr. Lincoln Turner[d]
Dr. Russell Anderson[d]
Dr. Angus Gray-Weale[f]
Dr. David Paganin[d]
Dr. Stuart Langley[g]
Dr. Willem van den Heuvel[e]
Dr. Marta Estrader[h]
Dr. James Walsh[b]
Dr. Chris Billington[d]
Dr. Michele Vonci[b]
Mr. Philip Chan[i]

[a] School of Chemistry, Monash University, Clayton, Victoria, Australia
[b] School of Chemistry, The University of Manchester, Manchester, United Kingdom
[c] Institut de Physique, Université de Liège, Belgium; Department of Chemistry, Missouri S&T, United States of America
[d] School of Physics, Monash University, Clayton, Victoria, Australia
[e] School of Chemistry, University of Melbourne, Victoria, Australia
[f] Bureau of Meteorology, Australia
[g] School of Chemistry, Manchester Metropolitan University, Manchester, United Kingdom
[h] School of Chemistry, Universitat de Barcelona, Catalonia, Spain
[i] Monash eResearch Centre, Monash University, Clayton, Victoria, Australia

1. Introduction

PHI is a computer package designed for the calculation and interpretation of the magnetic and spectroscopic properties of paramagnetic compounds. While the use of phenomenological Hamiltonians is not at all a new concept, *PHI* was conceived as a freely accessible and cross-platform program with wide functionality, new approaches and increased performance.

The program was designed, primarily, for the treatment of systems containing orbitally degenerate and strongly anisotropic ions, through the inclusion of Spin-Orbit (SO) coupling and Crystal-Field (CF) effects. Thus, *PHI* was written with the explicit inclusion of orbital angular momentum. The intra-atomic coulomb interaction is treated with the Russell-Saunders (or LS) formalism, such that only the total spin and the total orbital moments of the ground term are employed. Whilst designed for anisotropic calculations, *PHI* is also optimized for calculations involving magnetically isotropic or spin-only systems.

Another major design feature was to employ the Zeeman term in the Hamiltonian such that non-perturbative field dependent magnetic properties could be calculated. This also facilitates the calculation of field dependent properties such as Electron Paramagnetic Resonance (EPR) and Zeeman spectra.

One of the main goals is for the program to be approachable by non-experts; a goal that has been facilitated though the use of plain text input files and a Graphical User Interface (GUI) providing real-time visualization of data.

2. Theoretical Background

2.1 Notation

This manual uses the following notation for common mathematical quantities.

Table 2.1.1 – Mathematical notation

Quantity	**Symbol**
Scalar	A
Vector	$\vec{A}$
Vector component	A_α
Matrix	$\bar{\bar{A}}$
Matrix component	$A_{\alpha,\beta}$
Operator	$\hat{A}$
Vector operator	$\vec{\hat{A}}$
Vector operator component	$\hat{A}_\alpha$

2.2 Theory

For molecular ensembles in thermodynamic equilibrium, the underlying postulate is that each molecule possesses an electronic structure given by solution to the time independent Schrödinger equation, Equation 2.2.1. The action of the Hamiltonian operator, $\hat{H}$, on the wavefunction, Ψ, gives the energy of the state, E. The electronic wavefunction is usually separated into radial and angular parts and in the domain of spin Hamiltonians, the angular part is solved explicitly while the radial integrals become parameters to be determined. The Hilbert space for an individual molecule is constructed from the angular momentum basis states for each of N sites using either $|S_i, m_{S_i}\rangle$, $|J_i, m_{J_i}\rangle$ or $|L_i, m_{L_i}, S_i, m_{S_i}\rangle$ representations, where $i \in N$. Note: only a single term is used to describe each site, i.e. S_i, J_i or L_i and S_i are fixed. The total uncoupled basis of the system is the direct product of all the individual basis states, Equation 2.2.2. This system is solved by evaluating the matrix elements of the Hamiltonian over the basis states and diagonalizing the Hamiltonian matrix. The dimension of the Hilbert space and therefore the Hamiltonian matrix is given by Equation 2.2.3.

$$\hat{H}\Psi = E\Psi \tag{2.2.1}$$

$$|L, S, m_L, m_S\rangle = |L_1, S_1, m_{L_1}, m_{S_1}\rangle \otimes |L_2, S_2, m_{L_2}, m_{S_2}\rangle \otimes \dots |L_i, S_i, m_{L_i}, m_{S_i}\rangle,\ i \in N \tag{2.2.2}$$

$$dim = \prod_{i=1}^{N} (2L_i + 1)(2S_i + 1) \tag{2.2.3}$$

The Hamiltonian is composed of operators which act on the angular momentum basis functions to yield the matrix elements. The Hamiltonian is split into four components: the SO coupling, $\hat{H}_{SO}$, the exchange coupling, $\hat{H}_{EX}$, the CF interaction, $\hat{H}_{CF}$ and the Zeeman effect, $\hat{H}_{ZEE}$.

$$\hat{H} = \hat{H}_{SO} + \hat{H}_{EX} + \hat{H}_{CF} + \hat{H}_{ZEE} \tag{2.2.4}$$

Spin-orbit coupling

The SO coupling operator is usually given as Equation 2.2.5, however this first order model results in the SO multiplets following the Landé interval rule. This is correctly obeyed by ions of low atomic mass, such as the 3d ions, however deviations from the Landé interval rule for heavy ions due to term mixing by SO coupling are significant and must be accounted for. Thus in *PHI*, the SO operator is expanded as a power series following the parameterization of Karayianis,[1] Equation 2.2.6. The sum extends to order $2S_i$, where S_i is the total spin of the term in question. The coefficients, $\lambda_{1_i}, \lambda_{2_i}$ and λ_{3_i} were tabulated for the tripositive lanthanides by Karayianis, however we have optimized these and included higher orders where required,[2] Table 2.2.1.

$$\hat{H}_{SO} = \sum_{i=1}^{N} \lambda_i \left(\sigma_i \vec{\hat{L}}_i \cdot \vec{\hat{S}}_i\right) \tag{2.2.5}$$

$$\hat{H}_{SO} = \sum_{i=1}^{N} \sum_{j=1}^{2S_i} \lambda_{j_i} \left(\sigma_i \vec{\hat{L}}_i \cdot \vec{\hat{S}}_i\right)^j \tag{2.2.6}$$

where λ_{j_i} are the SO coupling constants

σ_i are the orbital reduction parameters

Table 2.2.1 – Optimized spin-orbit parameters for the triply ionized rare-earths

Ion		λ_1 (cm^{-1})	λ_2 (cm^{-1})	λ_3 (cm^{-1})	λ_4 (cm^{-1})	λ_5 (cm^{-1})	λ_6 (cm^{-1})
Ce^{III}	**Ref. 1**	640	-	-	-	-	-
	Opt.	691	-	-	-	-	-
Pr^{III}	**Ref. 1**	390	-4.63	-	-	-	-
	Opt.	421	-5.78	-	-	-	-
Nd^{III}	**Ref. 1**	299	-2.48	0.0475	-	-	-
	Opt.	326	-2.66	0.0247	-	-	-
Pm^{III}	**Ref. 1**	251	-1.99	0.0239	0	-	-
	Opt.	269	-1.85	0.00977	-0.000920	-	-
Sm^{III}	**Ref. 1**	228	-2.16	0.0368	0	0	-
	Opt.	241	-2.34	0.0315	-0.000743	-0.00000883	-
Eu^{III}	**Ref. 1**	214	-3.82	0.147	0	0	0
	Opt.	230	-3.28	0.269	0.000715	-0.00164	-0.000144

Tb^{III}	**Ref. 1**	-252	-4.50	-0.267	0	0	0
	Opt.	-260	0.997	0.223	-0.0402	-0.00685	-0.000267
Dy^{III}	**Ref. 1**	-357	-4.40	-0.121	0	0	-
	Opt.	-362	-2.73	-0.221	-0.00655	0.000110	-
Ho^{III}	**Ref. 1**	-497	-7.06	-0.139	0	-	-
	Opt.	-515	-7.83	-0.121	0.00629	-	-
Er^{III}	**Ref. 1**	-629	-18.2	-0.517	-	-	-
	Opt.	-572	-12.6	-1.85	-	-	-
Tm^{III}	**Ref. 1**	-875	-123	-	-	-	-
	Opt.	-684	-177	-	-	-	-
Yb^{III}	**Ref. 1**	-2910	-	-	-	-	-
	Opt.	-2957	-	-	-	-	-

Exchange coupling

For both spin-only and orbitally degenerate cases, the exchange Hamiltonian (Equation 2.2.7) is parameterized with the complete $\overline{\overline{J_{ij}}}$ tensor, Equation 2.2.8. In many cases this can be separated into two components; the (an)isotropic exchange (Equation 2.2.9) and the antisymmetric exchange (Equation 2.2.10), in which case $\overline{\overline{J_{ij}}}$ takes the form of Equation 2.2.11. While such an approach is commonplace in spin-only situations, the subject of magnetic exchange between orbitally degenerate ions is non-trivial and a number of attempts have been made to determine an effective operator for such cases.[3–7] Currently in *PHI*, the exchange interaction for orbitally degenerate ions follows the treatment of Lines,[8] which includes only the spin-spin interaction between the true spins in the $|L_i, m_{L_i}, S_i, m_{S_i}\rangle$ basis. In *PHI* however, the interaction can also be anisotropic and/or antisymmetric, thus is much more general than the original Lines model. The exchange coupling using the Lines approach may also be calculated in the $|J_i, m_{J_i}\rangle$ basis when used in conjunction with the lanthanide ions in the simple input method (see section 4.3), utilizing a Clebsch-Gordan decomposition.

By default the reference frame of the exchange matrix is coincident with the global coordinate system, however this can be rotated such that the anisotropic and antisymmetric interactions can be described in simple, local reference frames.

Note that upon swapping the site indices of the exchange Hamiltonian, the exchange tensor becomes its transpose, i.e. $\vec{\hat{S}}_i \cdot \overline{\overline{J_{ij}}} \cdot \vec{\hat{S}}_j = \vec{\hat{S}}_j \cdot \overline{\overline{J_{ij}}}^T \cdot \vec{\hat{S}}_i$.

Since version 3.0, nuclear spins can be included using the ****Ion block. In this case, the exchange parameters involving nuclear spins correspond to the hyperfine interactions. Note that the convention given here also applies to the nuclear spins, which is different to the usual hyperfine expression.

$$\hat{H}_{EX} = -2 \sum_{i \neq j}^{i,j \in N} \vec{\hat{S}}_i \cdot \overline{\overline{J_{ij}}} \cdot \vec{\hat{S}}_j \qquad (2.2.7)$$

$$\overline{\overline{J_{ij}}} = \begin{bmatrix} J_{ij_{xx}} & J_{ij_{xy}} & J_{ij_{xz}} \\ J_{ij_{yx}} & J_{ij_{yy}} & J_{ij_{yz}} \\ J_{ij_{zx}} & J_{ij_{zy}} & J_{ij_{zz}} \end{bmatrix} \tag{2.2.8}$$

$$\hat{H}_{(an)iso} = -2 \sum_{i \neq j}^{i,j \in N} J_{ij_x} \hat{S}_{i_x} \hat{S}_{j_x} + J_{ij_y} \hat{S}_{i_y} \hat{S}_{j_y} + J_{ij_z} \hat{S}_{i_z} \hat{S}_{j_z} \tag{2.2.9}$$

$$\hat{H}_{anti} = -2 \sum_{i \neq j}^{i,j \in N} \vec{d}_{ij} \cdot \left(\vec{\hat{S}}_i \times \vec{\hat{S}}_j \right)$$

$$= -2 \sum_{i \neq j}^{i,j \in N} d_{ij_x} \left(\hat{S}_{i_y} \hat{S}_{j_z} - \hat{S}_{i_z} \hat{S}_{j_y} \right) + d_{ij_y} \left(\hat{S}_{i_z} \hat{S}_{j_x} - \hat{S}_{i_x} \hat{S}_{j_z} \right) + d_{ij_z} \left(\hat{S}_{i_x} \hat{S}_{j_y} - \hat{S}_{i_y} \hat{S}_{j_x} \right)$$

$$(2.2.10)$$

$$\overline{\overline{J_{ij}}} = \begin{bmatrix} J_{ij_x} & d_{ij_z} & -d_{ij_y} \\ -d_{ij_z} & J_{ij_y} & d_{ij_x} \\ d_{ij_y} & -d_{ij_x} & J_{ij_z} \end{bmatrix} \tag{2.2.11}$$

Crystal-field potential

The CF potential is constructed from spherical harmonics to represent the environment in which the spin carrier resides. While twenty-seven terms exist in the full expansion, the number required may be reduced as the CF Hamiltonian must be invariant under the operations of the point group of the molecule (see below for a brief outline of the rules for non-zero parameters). Many approaches have been attempted over the years to determine Crystal-Field Parameters (CFPs), such as the Point Charge (PCM),[9] Angular Overlap (AOM)[10,11] and Superposition (SM)[12] models, however all have fallen short of consistently predicting these parameters. This is because, in reality, the electrostatic CF is inadequate due to the overlooked contributions from covalency, non-orthogonality, screening and polarization of the orbitals.[13] In spite of these criticisms, the CF model succeeds in describing experimental results when it is considered a phenomenological Hamiltonian, where the resultant parameters have no direct physical interpretation. Given this interpretation and the close similarity of the operators (see below), the CF Hamiltonian is also used in *PHI* to model Zero Field Splittings (ZFS) of effective spins.

There are numerous parameterization schemes for the effective CF Hamiltonian and care must be taken to avoid confusion. For a good grounding, see Mulak and Gajek[13], Hutchings[9] and Rudowicz.[14] As *PHI* constructs the Hamiltonian within a total spin-orbit basis, the operator equivalent technique of Stevens *et al.*[15,16] was chosen as the most efficient method for the evaluation of matrix elements, even though the notation is less transparent than others, Equation 2.2.12. Here, the definitions of the $\hat{O}_k^q$ operators are consistent with Hutchings,[9] Mulak and Gajek[13] and Stevens,[16] however for clarity definitions of all the positive and negative operators are given below in Table 2.2.2. The operator equivalents themselves are polynomials of angular momentum operators, derived from the tesseral harmonics and *PHI* includes all even, odd, positive and negative orders (q) for the 2nd, 4th and 6th rank (k) operators. The rank, k, is restricted to $k = 2$, $k = 4$ and $k = 6$ as only the ground terms of the ground configuration are considered. The use of the negative q operators is equivalent to the ‘sine’ type operators of Hutchings[9] and the ‘imaginary’ CFPs in Wybourne notation.[13] The method relies on the use of the operator equivalent factors, θ_k, to relate the total angular momentum matrix elements to the single electron matrix elements. These factors have been tabulated for the ground multiplets for all lanthanides,[17] but not as far as the author is aware for the ground *terms* of the lanthanides; these are now presented in Table 2.2.4. The operator equivalent factors are automatically included for the lanthanide ions when using the simple input method (*****Ion* block), however are subsumed by the relevant CFPs in all other cases.

In *PHI*, the CF Hamiltonian is applied to either the orbital or the total angular momentum components of a given centre. That is, if the centre possesses a non-zero orbital moment the CF Hamiltonian directly acts on the orbital component as a true CF. However, if the centre does not possess an orbital moment, the CF Hamiltonian acts on the effective spin or total angular momentum, depending on one’s interpretation of the assigned ‘spin’. Note that the orbital reduction parameter, σ_i, is only relevant when the CF Hamiltonian is applied to an orbital moment directly.

$$\hat{H}_{CF} = \sum_{i=1}^{N} \sum_{k=2,4,6} \sum_{q=-k}^{k} {\sigma_i}^{k} {B_k^q}_i \theta_k {\hat{O}_k^q}_i \tag{2.2.12}$$

where σ_i are the orbital reduction parameters
${B_k^q}_i$ are the CFPs (${A_k^q}_i \langle r^k \rangle_i$ in Steven’s notation)
θ_k are the operator equivalent factors
${\hat{O}_k^q}_i$ are operator equivalents

Table 2.2.2 – Definition of the Stevens operators

Operator
$\hat{O}_2^{-2} = \frac{-i}{2}\left({\hat{L}_+}^2 - {\hat{L}_-}^2\right)$
$\hat{O}_2^{-1} = \frac{-i}{4}\left(\hat{L}_z(\hat{L}_+ - \hat{L}_-) + (\hat{L}_+ - \hat{L}_-)\hat{L}_z\right)$
$\hat{O}_2^{0} = 3{\hat{L}_z}^2 - \hat{L}^2$
$\hat{O}_2^{+1} = \frac{1}{4}\left(\hat{L}_z(\hat{L}_+ + \hat{L}_-) + (\hat{L}_+ + \hat{L}_-)\hat{L}_z\right)$
$\hat{O}_2^{+2} = \frac{1}{2}\left({\hat{L}_+}^2 + {\hat{L}_-}^2\right)$
$\hat{O}_4^{-4} = \frac{-i}{2}\left({\hat{L}_+}^4 - {\hat{L}_-}^4\right)$

$$\hat{O}_4^{-3} = \frac{-i}{4}\left(\hat{L}_z\left(\hat{L}_+{}^3 - \hat{L}_-{}^3\right) + \left(\hat{L}_+{}^3 - \hat{L}_-{}^3\right)\hat{L}_z\right)$$

$$\hat{O}_4^{-2} = \frac{-i}{4}\left(\left(7\hat{L}_z{}^2 - \hat{L}^2 - 5\right)\left(\hat{L}_+{}^2 - \hat{L}_-{}^2\right) + \left(\hat{L}_+{}^2 - \hat{L}_-{}^2\right)\left(7\hat{L}_z{}^2 - \hat{L}^2 - 5\right)\right)$$

$$\hat{O}_4^{-1} = \frac{-i}{4}\left(\left(7\hat{L}_z{}^3 - 3\hat{L}^2\hat{L}_z - \hat{L}_z\right)\left(\hat{L}_+ - \hat{L}_-\right) + \left(\hat{L}_+ - \hat{L}_-\right)\left(7\hat{L}_z{}^3 - 3\hat{L}^2\hat{L}_z - \hat{L}_z\right)\right)$$

$$\hat{O}_4^{0} = 35\hat{L}_z{}^4 - 30\hat{L}^2\hat{L}_z{}^2 + 25\hat{L}_z{}^2 + 3\hat{L}^{2^2} - 6\hat{L}^2$$

$$\hat{O}_4^{+1} = \frac{1}{4}\left(\left(7\hat{L}_z{}^3 - 3\hat{L}^2\hat{L}_z - \hat{L}_z\right)\left(\hat{L}_+ + \hat{L}_-\right) + \left(\hat{L}_+ + \hat{L}_-\right)\left(7\hat{L}_z{}^3 - 3\hat{L}^2\hat{L}_z - \hat{L}_z\right)\right)$$

$$\hat{O}_4^{+2} = \frac{1}{4}\left(\left(7\hat{L}_z{}^2 - \hat{L}^2 - 5\right)\left(\hat{L}_+{}^2 + \hat{L}_-{}^2\right) + \left(\hat{L}_+{}^2 + \hat{L}_-{}^2\right)\left(7\hat{L}_z{}^2 - \hat{L}^2 - 5\right)\right)$$

$$\hat{O}_4^{+3} = \frac{1}{4}\left(\hat{L}_z\left(\hat{L}_+{}^3 + \hat{L}_-{}^3\right) + \left(\hat{L}_+{}^3 + \hat{L}_-{}^3\right)\hat{L}_z\right)$$

$$\hat{O}_4^{+4} = \frac{1}{2}\left(\hat{L}_+{}^4 + \hat{L}_-{}^4\right)$$

$$\hat{O}_6^{-6} = \frac{-i}{2}\left(\hat{L}_+{}^6 - \hat{L}_-{}^6\right)$$

$$\hat{O}_6^{-5} = \frac{-i}{4}\left(\left(\hat{L}_+{}^5 - \hat{L}_-{}^5\right)\hat{L}_z + \hat{L}_z\left(\hat{L}_+{}^5 - \hat{L}_-{}^5\right)\right)$$

$$\hat{O}_6^{-4} = \frac{-i}{4}\left(\left(\hat{L}_+{}^4 - \hat{L}_-{}^4\right)\left(11\hat{L}_z{}^2 - \hat{L}^2 - 38\right) + \left(11\hat{L}_z{}^2 - \hat{L}^2 - 38\right)\left(\hat{L}_+{}^4 - \hat{L}_-{}^4\right)\right)$$

$$\begin{aligned}\hat{O}_6^{-3} = \frac{-i}{4}\Big(&\left(\hat{L}_+{}^3 - \hat{L}_-{}^3\right)\left(11\hat{L}_z{}^3 - 3\hat{L}^2\hat{L}_z - 59\hat{L}_z\right)\\ &+ \left(11\hat{L}_z{}^3 - 3\hat{L}^2\hat{L}_z - 59\hat{L}_z\right)\left(\hat{L}_+{}^3 - \hat{L}_-{}^3\right)\Big)\end{aligned}$$

$$\begin{aligned}\hat{O}_6^{-2} = \frac{-i}{4}\Big(&\left(\hat{L}_+{}^2 - \hat{L}_-{}^2\right)\left(33\hat{L}_z{}^4 - 18\hat{L}^2\hat{L}_z{}^2 - 123\hat{L}_z{}^2 + \hat{L}^{2^2} + 10\hat{L}^2 + 102\right)\\ &+ \left(33\hat{L}_z{}^4 - 18\hat{L}^2\hat{L}_z{}^2 - 123\hat{L}_z{}^2 + \hat{L}^{2^2} + 10\hat{L}^2 + 102\right)\left(\hat{L}_+{}^2 - \hat{L}_-{}^2\right)\Big)\end{aligned}$$

$$\begin{aligned}\hat{O}_6^{-1} = \frac{-i}{4}\Big(&\left(\hat{L}_+ - \hat{L}_-\right)\left(33\hat{L}_z{}^5 - 30\hat{L}^2\hat{L}_z{}^3 + 15\hat{L}_z{}^3 + 5\hat{L}^{2^2}\hat{L}_z - 10\hat{L}^2\hat{L}_z + 12\hat{L}_z\right)\\ &+ \left(33\hat{L}_z{}^5 - 30\hat{L}^2\hat{L}_z{}^3 + 15\hat{L}_z{}^3 + 5\hat{L}^{2^2}\hat{L}_z - 10\hat{L}^2\hat{L}_z + 12\hat{L}_z\right)\left(\hat{L}_+ - \hat{L}_-\right)\Big)\end{aligned}$$

$$\begin{aligned}\hat{O}_6^{0} = 231\hat{L}_z{}^6 - 315\hat{L}^2\hat{L}_z{}^4 + 735\hat{L}_z{}^4 + 105\hat{L}^{2^2}\hat{L}_z{}^2 - 525\hat{L}^2\hat{L}_z{}^2 + 294\hat{L}_z{}^2 - 5\hat{L}^{2^3} + 40\hat{L}^{2^2}\\ - 60\hat{L}^2\end{aligned}$$

$$\begin{aligned}\hat{O}_6^{+1} = \frac{1}{4}\Big(&\left(\hat{L}_+ + \hat{L}_-\right)\left(33\hat{L}_z{}^5 - 30\hat{L}^2\hat{L}_z{}^3 + 15\hat{L}_z{}^3 + 5\hat{L}^{2^2}\hat{L}_z - 10\hat{L}^2\hat{L}_z + 12\hat{L}_z\right)\\ &+ \left(33\hat{L}_z{}^5 - 30\hat{L}^2\hat{L}_z{}^3 + 15\hat{L}_z{}^3 + 5\hat{L}^{2^2}\hat{L}_z - 10\hat{L}^2\hat{L}_z + 12\hat{L}_z\right)\left(\hat{L}_+ + \hat{L}_-\right)\Big)\end{aligned}$$

$$\begin{aligned}\hat{O}_6^{+2} = \frac{1}{4}\Big(&\left(\hat{L}_+{}^2 + \hat{L}_-{}^2\right)\left(33\hat{L}_z{}^4 - 18\hat{L}^2\hat{L}_z{}^2 - 123\hat{L}_z{}^2 + \hat{L}^{2^2} + 10\hat{L}^2 + 102\right)\\ &+ \left(33\hat{L}_z{}^4 - 18\hat{L}^2\hat{L}_z{}^2 - 123\hat{L}_z{}^2 + \hat{L}^{2^2} + 10\hat{L}^2 + 102\right)\left(\hat{L}_+{}^2 + \hat{L}_-{}^2\right)\Big)\end{aligned}$$

$\hat{O}_6^{+3} = \frac{1}{4}\left(\left(\hat{L}_+{}^3 + \hat{L}_-{}^3\right)\left(11\hat{L}_z{}^3 - 3\hat{L}^2\hat{L}_z - 59\hat{L}_z\right) + \left(11\hat{L}_z{}^3 - 3\hat{L}^2\hat{L}_z - 59\hat{L}_z\right)\left(\hat{L}_+{}^3 + \hat{L}_-{}^3\right)\right)$
$\hat{O}_6^{+4} = \frac{1}{4}\left(\left(\hat{L}_+{}^4 + \hat{L}_-{}^4\right)\left(11\hat{L}_z{}^2 - \hat{L}^2 - 38\right) + \left(11\hat{L}_z{}^2 - \hat{L}^2 - 38\right)\left(\hat{L}_+{}^4 + \hat{L}_-{}^4\right)\right)$
$\hat{O}_6^{+5} = \frac{1}{4}\left(\left(\hat{L}_+{}^5 + \hat{L}_-{}^5\right)\hat{L}_z + \hat{L}_z\left(\hat{L}_+{}^5 + \hat{L}_-{}^5\right)\right)$
$\hat{O}_6^{+6} = \frac{1}{2}\left(\hat{L}_+{}^6 + \hat{L}_-{}^6\right)$

Table 2.2.3 – Operator equivalent factors for the lanthanides in the $|J, m_J\rangle$ basis

Ion	Multiplet	2nd Rank	4th Rank	6th Rank
Ce$^{\text{III}}$	^{2}F$_{5/2}$	-2/35	2/315	0
Pr$^{\text{III}}$	^{3}H$_{4}$	-52/2475	-4/5445	272/4459455
Nd$^{\text{III}}$	^{4}I$_{9/2}$	-7/1089	-136/467181	-1615/42513471
Pm$^{\text{III}}$	^{5}I$_{4}$	14/1815	952/2335905	2584/42513471
Sm$^{\text{III}}$	^{6}H$_{5/2}$	13/315	26/10395	0
Eu$^{\text{III}}$	^{7}F$_{0}$	0	0	0
Gd$^{\text{III}}$	^{8}S$_{7/2}$	0	0	0
Tb$^{\text{III}}$	^{7}F$_{6}$	-1/99	2/16335	-1/891891
Dy$^{\text{III}}$	^{6}H$_{15/2}$	-2/315	-8/135135	4/3864861
Ho$^{\text{III}}$	^{5}I$_{8}$	-1/450	-1/30030	-5/3864861
Er$^{\text{III}}$	^{4}I$_{15/2}$	4/1575	2/45045	8/3864861
Tm$^{\text{III}}$	^{3}H$_{6}$	1/99	8/49005	-5/891891
Yb$^{\text{III}}$	^{2}F$_{7/2}$	2/63	-2/1155	4/27027

Table 2.2.4 – Operator equivalent factors for the lanthanides in the $|L, m_L, S, m_S\rangle$ basis

Ion	Term	2nd Rank	4th Rank	6th Rank
Ce$^{\text{III}}$	^{2}F	-2/45	2/495	-4/3861
Pr$^{\text{III}}$	^{3}H	-2/135	-4/10395	2/81081
Nd$^{\text{III}}$	^{4}I	-2/495	-2/16335	-10/891891
Pm$^{\text{III}}$	^{5}I	2/495	2/16335	10/891891
Sm$^{\text{III}}$	^{6}H	2/135	4/10395	-2/81081
Eu$^{\text{III}}$	^{7}F	2/45	-2/495	4/3861
Gd$^{\text{III}}$	^{8}S	0	0	0
Tb$^{\text{III}}$	^{7}F	-2/45	2/495	-4/3861
Dy$^{\text{III}}$	^{6}H	-2/135	-4/10395	2/81081
Ho$^{\text{III}}$	^{5}I	-2/495	-2/16335	-10/891891
Er$^{\text{III}}$	^{4}I	2/495	2/16335	10/891891
Tm$^{\text{III}}$	^{3}H	2/135	4/10395	-2/81081
Yb$^{\text{III}}$	^{2}F	2/45	-2/495	4/3861

Note that only 2nd and 4th rank operators are required to describe CFs for d-block ions, whereas the 6th rank is also, generally, required for f-block ions. Of course, however, higher rank operators may be required to accurately describe ZFS effects.

In cubic symmetry (*e.g.* O_h or T_d) the B_4^4 and B_6^4 terms are non-zero and directly related to the axial B_4^0 and B_6^0 terms (Equations 2.2.13 and 2.2.14).[13] These relations can be enforced by *PHI*, by using the *force_cubic* command, such that only the B_4^0 and B_6^0 terms need to be specified (this is particularly useful when fitting). In this convention for *d*-block ions, $B_4^0 > 0$ corresponds to T_d symmetry and $B_4^0 < 0$ corresponds to O_h symmetry.

$$B_4^4 = 5B_4^0 \tag{2.2.13}$$

$$B_6^4 = -21B_6^0 \tag{2.2.14}$$

The second order CF operators are intimately related to those of the standard ZFS Spin Hamiltonian[17] and using the definitions of the CF operators as in Table 2.2.2, the relationships between the ZFS parameters and the CFPs are therefore expressed in Equations 2.2.15 and 2.2.16.

$$D = 3B_2^0\theta_2 \tag{2.2.15}$$

$$E = B_2^2\theta_2 \tag{2.2.16}$$

The non-zero CFPs are determined solely by the point group of the ion in question. Often the assumed point group symmetry does not include the entire molecule, but only the first coordination sphere of the paramagnetic ion, as this is the largest contribution to the perturbation. Often, idealized symmetry may be used initially, followed by small corrections to allow for distortions of lower symmetry. For a full C_1 representation, all 27 CFPs are required. If the group is not C_1 then only CFPs with even q are required. If a C_n axis is present, only CFPs with $q = jn$, where j is an integer, are required. Only the following groups need negative q CFPs: C_1, C_i (S_2), C_3, C_{3i} (S_6), C_4, S_4 and C_6. A comprehensive list of non-zero CFPs for all point group symmetries can be found in Gorller-Walrand and Binnemans' chapter.[18]

Since version 3.0, nuclear spins can be included using the ****Ion block. In this case, the CFPs involving nuclear spins correspond to the quadrupole splitting. Note that the convention given above also applies to the nuclear spins, which is different to the usual quadrupole expression.

Zeeman Effect

The Zeeman Effect is the stabilization and destabil1ization of angular momentum projections parallel and anti-parallel to a magnetic field, Equation 2.2.17. It is this response to the magnetic field which is responsible for the observable magnetic properties, such as magnetization and magnetic susceptibility.

Since version 3.0, nuclear spins can be included using the ****Ion block. In this case, the Zeeman term for nuclear spins is implemented by using the effective g-values given in Table 4.3.1.

$$\hat{H}_{ZEE} = \mu_B \sum_{i=1}^{N} \left(\sigma_i \vec{\hat{L}}_i \cdot \bar{\bar{I}} + \vec{\hat{S}}_i \cdot \bar{\bar{g}}_i \right) \cdot \vec{B} \tag{2.2.17}$$

where $\bar{\bar{I}}$ is the identity matrix
$\bar{\bar{g}}_i$ is the g-tensor

Orbital reduction factor

Note that in all Hamiltonians above, the σ parameter has been included with all orbital operators. This is the combined $\sigma = -A \cdot \kappa$ factor, required when using the T≡P equivalence for orbital triplet terms.[19] A is required when making the T → P substitution and takes the value of 1.0 when representing a T_2 term and 3/2 when representing a T_1 term. κ (or k in some texts) is the orbital reduction factor which is an empirical constant, $0 < \kappa < 1$, and accounts for a reduction in the effective orbital angular momentum due to covalency or low symmetry effects. It can be effectively removed setting σ to unity (default). Note that for the SO and CF Hamiltonians the orbital reduction factor is included as σ_i, ${\sigma_i}^2$, ${\sigma_i}^3$, ${\sigma_i}^4$, ${\sigma_i}^5$ or ${\sigma_i}^6$ for first, second, third, fourth, fifth and sixth rank, respectively, where required.

Magnetic properties

The inclusion of the Zeeman Hamiltonian allows the magnetic properties to be calculated from first principles[20] without resorting to perturbation theory. Thus, full mixing of all states by the magnetic field is implicitly included. The fundamental definitions for the magnetic properties are expressed in Equations 2.2.18 and 2.2.19.

$$M \propto -\frac{\partial E}{\partial B} \tag{2.2.18}$$

$$\chi \propto \frac{\partial M}{\partial B} \tag{2.2.19}$$

The molar magnetization is the sum of the magnetization of each state weighted by its Boltzmann population, Equation 2.2.20, where Z is the partition function, Equation 2.2.22, giving the magnetization for a single Cartesian direction, $\alpha \in \mathrm{x, y, z}$, in Bohr Magnetons per mole (μ_B mol^{-1}). Equivalently, the Magnetization can be calculated using Equation 2.2.21.

$$M_\alpha = \frac{1}{Z\mu_B} \sum_{i=1}^{dim} -\frac{\partial E_i}{\partial B_\alpha} e^{\frac{-E_i}{k_B T}} \tag{2.2.20}$$

$$M_\alpha = \frac{k_B T}{\mu_B} \frac{\partial \ln Z}{\partial B_\alpha} \tag{2.2.21}$$

$$Z = \sum_{i=1}^{dim} e^{\frac{-E_i}{k_B T}} \tag{2.2.22}$$

Following Equation 2.2.19, the molar magnetic susceptibility is the first derivative of Equation 2.2.20, resulting in Equation 2.2.23, which contains terms that depend on the first and second derivatives of the eigenvalues with respect to the magnetic field. As there are two derivative steps there are nine possible combinations of the Cartesian directions, $\alpha, \beta \in x, y, z$, leading to the definition of the 3×3 magnetic susceptibility tensor. Equation 2.2.23 reduces to the traditional vanVleck formula in the limit of zero magnetic field, however the numerical method employed here is capable of accurately determining the susceptibility in the presence of non-zero fields as used in experiment. Following Equation 2.2.21, Equation 2.2.24 is entirely equivalent to Equation 2.2.23.

$$\chi_{\alpha,\beta} = \frac{\partial M_\alpha}{\partial B_\beta} = \frac{N_A}{10 k_B T Z^2}\left[Z\left(\sum_{i=1}^{dim} \frac{\partial E_i}{\partial B_\alpha}\frac{\partial E_i}{\partial B_\beta} e^{\frac{-E_i}{k_B T}} - k_B T \sum_{i=1}^{dim} \frac{\partial^2 E_i}{\partial B_\alpha \partial B_\beta} e^{\frac{-E_i}{k_B T}}\right) \right. \\ \left. - \left(\sum_{i=1}^{dim} \frac{\partial E_i}{\partial B_\alpha} e^{\frac{-E_i}{k_B T}}\right)\left(\sum_{i=1}^{dim} \frac{\partial E_i}{\partial B_\beta} e^{\frac{-E_i}{k_B T}}\right)\right]$$

(2.2.23)

$$\chi_{\alpha,\beta} = \frac{N_A k_B T}{10}\frac{\partial^2 \ln Z}{\partial B_\alpha \partial B_\beta} \tag{2.2.24}$$

Most commonly however, the magnetic susceptibility as measured is actually approximated as $\chi \approx M/B$. While the difference between this approximation and the true differential susceptibility given by Equations 2.2.23 and 2.2.24 is minimal for isotropic cases, it can be significant for highly anisotropic systems. Therefore by default since version 3.0, *PHI* calculates the magnetic susceptibility using Equation 2.2.25 – calculation of the differential susceptibility can still be activated by keyword. Since version 3.1.2 *PHI* can calculate the full magnetic susceptibility tensor, and it does do using the differential formula of Equation 2.2.24.

$$\chi_\alpha = \frac{k_B T}{\mu_B}\frac{\partial \ln Z}{\partial B_\alpha}\frac{1}{B_\alpha} \tag{2.2.25}$$

The entropy change associated with the application and removal of a magnetic field is the quantity associated with the Magnetocaloric Effect (MCE). The magnetic entropy change is easily calculated for isotropic or anisotropic systems through Equation 2.2.26.[21] Note that M_r is the molecular mass of the complex and the entropy change is in units of J kg^{-1} K^{-1}.

$$-\Delta S_\alpha = \frac{-1000 N_A}{M_r} \int_{B_\alpha=0}^{B_\alpha=\Delta B} \frac{\partial M_\alpha}{\partial T} dB_\alpha \tag{2.2.26}$$

The low temperature heat capacity of a paramagnetic system can be very sensitive to the magnetic interactions. *PHI* is equipped to calculate the magnetic heat capacity through Equation 2.2.27, which includes a phenomenological term to capture the effect of the lattice heat capacity.[22] The heat capacity is given in units of R ($N_A k_B$), where T_D is the Debye temperature and α is the lattice exponent.

$$C = \frac{Z\left(\sum_{i=1}^{dim} {E_i}^2 e^{\frac{-E_i}{k_B T}}\right) - \left(\sum_{i=1}^{dim} E_i e^{\frac{-E_i}{k_B T}}\right)^2}{{k_B}^2 T^2 Z^2} + 234\left(\frac{T}{T_D}\right)^\alpha \tag{2.2.27}$$

Approximations

Whilst the general method for the calculation of the magnetic properties of arbitrary systems has been given above, a useful simplification of the method is possible when considering magnetically isotropic ‘spin-only’ compounds. Taking advantage of the spherical symmetry of the Hamiltonian in conjunction with first order approximation methods can lead to a substantial reduction in the computational demands of the problem. While the uncoupled basis is most useful for anisotropic systems easily allowing formulation of the SO and CF Hamiltonians, isotropic systems requiring only the isotropic exchange Hamiltonian are block diagonal in a total spin basis. In this case the problem can be solved by considering each block independently, greatly reducing the dimension of the problem and speeding up the calculation. The matrix elements can be calculated using Irreducible Tensor Operators (ITOs) and the Wigner-Ekhart theorem and while the literature is well established, the necessary equations and procedures are presented to clarify frequent typographical errors and to present a consistent notation.

In this example, the coupled basis is formed by first coupling S_1 and S_2 to make S_{12} or $\tilde{S}_1$, followed by coupling $\tilde{S}_1$ to S_3 to make S_{123} or $\tilde{S}_2$ etc., to the final total spin S, expressed in bra-ket notation in Equation 2.2.28. Recall that these are vector sums such that Equation 2.2.29 must be satisfied for all coupling steps.

$$\left|S_1, S_2, \tilde{S}_1, S_3, \tilde{S}_2, \dots, S, m_S\right\rangle \equiv \left|\left(\tilde{S}\right), S, m_S\right\rangle \tag{2.2.28}$$

$$\left|S_i - S_j\right| \leq \tilde{S}_k \leq S_i + S_j \tag{2.2.29}$$

The isotropic exchange Hamiltonian can be represented by use of a 0th rank tensor operator,[23] Equation 2.2.30. The matrix elements of spherical tensor operators are evaluated by applying the Wigner-Ekhart theorem[24] followed by a decoupling procedure to calculate the reduced matrix elements,[25,26] as expressed in Equation 2.2.31, where the numerator of the fraction is a Clebsch-Gordan coefficient and the quantities in braces are Wigner 9j symbols[27] (see below for simplifications). The remaining reduced matrix element can be easily calculated (see below). Note that the k_i and $\tilde{k}_i$ values are the ranks of the component and intermediate spins, respectively, and can be easily determined using simple rules.[26]

$$\hat{H}_{EX} = -2 \sum_{i<j}^{i,j \in N} J_{ij} \left(\vec{\hat{S}}_i \cdot \vec{\hat{S}}_j \right) = 2\sqrt{3} \sum_{i<j}^{i,j \in N} J_{ij} \hat{T}^{(0)} \tag{2.2.30}$$

$$\begin{gathered} \left\langle (\tilde{S}'), S', m_S' \middle| \hat{T}^{(0)} \middle| (\tilde{S}), S, m_S \right\rangle \\ = \frac{\langle S, m_S; 0,0 | S', m_S' \rangle}{\sqrt{2S'+1}} \sqrt{\left(2\tilde{k}_1+1\right)\left(2\tilde{S}_1+1\right)\left(2\tilde{S}_1'+1\right)} \begin{Bmatrix} S_1 & S_1 & k_1 \\ S_2 & S_2 & k_2 \\ \tilde{S}_1' & \tilde{S}_1 & \tilde{k}_1 \end{Bmatrix} \\ \times \left(\prod_{i=1}^{N} \langle S_i || \, \hat{S}^{(k_i)} \, || S_i \rangle \right) \left(\prod_{i=2}^{N-1} \sqrt{\left(2\tilde{k}_i+1\right)\left(2\tilde{S}_i+1\right)\left(2\tilde{S}_i'+1\right)} \begin{Bmatrix} \tilde{S}_{i-1}' & \tilde{S}_{i-1} & \tilde{k}_{i-1} \\ S_{i+1} & S_{i+1} & k_{i+1} \\ \tilde{S}_i' & \tilde{S}_i & \tilde{k}_i \end{Bmatrix} \right) \end{gathered} \tag{2.2.31}$$

As the tensor is rank zero, the Clebsch-Gordan coefficient is equivalent to two Kronecker delta functions, Equation 2.2.32. While this simplifies the calculations, it also implies something much more meaningful – there is no dependence on the magnetic quantum number at all, such that it may be excluded from the basis and the dimensionality of the Hamiltonian matrix further reduced. Coupled with block diagonalization of the matrix, this leads to a tremendous reduction in the computational effort required for the problem.

$$\langle S, m_S; 0,0 | S', m_S' \rangle = \delta_{S,S'} \delta_{m_S, m_S'} \tag{2.2.32}$$

The occurrence of Wigner 9j symbols in every matrix element is unfortunate due to their computational complexity, however in this case there are only four possible 9j symbols which are easily simplified.[26] They are presented below in Equations 2.2.33 – 2.2.36, where the quantities in the braces on the right hand side of the equations are Wigner 6j symbols.

$$\begin{Bmatrix} a & b & 0 \\ c & d & 0 \\ e & f & 0 \end{Bmatrix} = \frac{\delta_{a,b}\delta_{c,d}\delta_{e,f}}{\sqrt{(2a+1)(2c+1)(2e+1)}} \tag{2.2.33}$$

$$\begin{Bmatrix} a & b & 1 \\ c & d & 0 \\ e & f & 0 \end{Bmatrix} = \frac{\delta_{c,d}(-1)^{a+f+c+1}}{\sqrt{3(2c+1)}} \begin{Bmatrix} b & a & 1 \\ e & f & c \end{Bmatrix} \tag{2.2.34}$$

$$\begin{Bmatrix} a & b & 1 \\ c & d & 1 \\ e & f & 0 \end{Bmatrix} = \frac{\delta_{e,f}(-1)^{b+c+e+1}}{\sqrt{3(2e+1)}} \begin{Bmatrix} a & b & 1 \\ d & c & e \end{Bmatrix} \tag{2.2.35}$$

$$\begin{Bmatrix} a & b & 0 \\ c & d & 1 \\ e & f & 1 \end{Bmatrix} = \frac{\delta_{a,b}(-1)^{a+d+e+1}}{\sqrt{3(2a+1)}} \begin{Bmatrix} f & e & 1 \\ c & d & a \end{Bmatrix} \tag{2.2.36}$$

The reduced matrix elements remaining in Equation 2.2.31 are easily calculated, depending on the rank of the particular spin operator:[25]

$$\langle S_i || \hat{S}^{(0)} || S_i \rangle = \sqrt{2S_i + 1} \tag{2.2.37}$$

$$\langle S_i || \hat{S}^{(1)} || S_i \rangle = \sqrt{S(S+1)(2S+1)} \tag{2.2.38}$$

Once the matrix elements have been calculated, the matrix is diagonalized to determine the eigenvalues and eigenvectors of the coupled states. To evaluate the magnetic properties it is necessary to determine the effective g-factors for the coupled spin multiplets. In general, the spin multiplets, ψ_a, originate from a mixture of the different $|(\tilde{S}), S_a\rangle$ coupled basis states, necessitating further ITO algebra.[28] The g-factors for each multiplet can be calculated according to Equations 2.2.39 – 2.2.41, where the spin projection coefficients $p_{a,i}$ represent the effective spin density of the $|(\tilde{S}), S_a\rangle$ on the ith metal site and the $c_{a,\tilde{S}'}$ factors are the components of the eigenvector describing state ψ_a. Note that this procedure is very slow for large systems, and can be avoided if a single g-factor is used for all sites. With the g-factors known, the magnetic properties are calculated by considering the first order Zeeman perturbation to the m_S states.

$$g_a = \sum_{i=1}^{N} p_{a,i} g_i \tag{2.2.39}$$

$$p_{a,i} = \frac{b_{a,i}}{\sqrt{S_a(S_a+1)(2S_a+1)}} \tag{2.2.40}$$

$$\begin{aligned} b_{a,i} &= \sum_{\tilde{S}'} \sum_{\tilde{S}} c_{a,\tilde{S}'} c_{a,\tilde{S}} \left\langle (\tilde{S}'), S \middle\| \hat{S}^{(k_i)} \middle\| (\tilde{S}), S \right\rangle \\ &= \sum_{\tilde{S}'} \sum_{\tilde{S}} c_{a,\tilde{S}'} c_{a,\tilde{S}} \sqrt{(2\tilde{k}_1+1)(2\tilde{S}_1+1)(2\tilde{S}_1'+1)} \begin{Bmatrix} S_1 & S_1 & k_1 \\ S_2 & S_2 & k_2 \\ \tilde{S}_1' & \tilde{S}_1 & \tilde{k}_1 \end{Bmatrix} \\ &\times \left(\prod_{i=1}^{N} \langle S_i || \hat{S}^{(k_i)} || S_i \rangle \right) \left(\prod_{i=2}^{N-1} \sqrt{(2\tilde{k}_i+1)(2\tilde{S}_i+1)(2\tilde{S}_i'+1)} \begin{Bmatrix} \tilde{S}_{i-1}' & \tilde{S}_{i-1} & \tilde{k}_{i-1} \\ S_{i+1} & S_{i+1} & k_{i+1} \\ \tilde{S}_i' & \tilde{S}_i & \tilde{k}_i \end{Bmatrix} \right) \end{aligned} \tag{2.2.41}$$

Powder integration

For powder measurements on anisotropic systems, the calculations must be integrated over many orientations to accurately reflect the experiment. While poly-crystalline samples contain a finite number of crystallites with discrete orientations, it is usually assumed that the size of the crystals is small enough that it is closely representative of a powder sample with an infinite number of orientations evenly distributed on the sphere. For the magnetic susceptibility, it is sufficient to use the ‘*xyz*’ integration scheme, as this is exact for a second rank tensor property. For the magnetization however, the ‘*xyz*’ scheme is inadequate and should not be used. A number of orientation integration schemes are possible; *PHI* uses the Zaremba-Conroy-Wolfsberg (ZCW) scheme as presented by Levitt.[29] The implementation in *PHI* samples the magnetic properties over a hemisphere, as magnetic properties are invariant under inversion of the magnetic field.

Pseudo g-tensors

For calculations involving anisotropic ions which give rise to doublet states, pseudo g-tensors may be calculated within the basis of each doublet. This is equivalent to treating each doublet as a pseudo-spin $\tilde{S} = 1/2$ state whose magnetic anisotropy is given by the g-tensor. For Kramers systems these doublets are related by time inversion symmetry and the treatment is rigorous, however for non-Kramers systems the g-tensors for pseudo doublets are only approximate and only g_z is non-zero due to vanishing off-diagonal elements between the conjugate states.[17] The theory is well established,[30,31] but a brief overview of the method will be given. Note that *PHI* does not currently support the g-tensor calculation in bases of other values of pseudo-spin.

For a given system, the expectation values of the three Cartesian magnetic moment operators are evaluated in the basis of the zero field wavefunction, Equation 2.2.42. The g-tensor is then constructed for each doublet through Equation 2.2.43, where ψ and ψ' are the wavefunctions of the doublet and $\alpha, \beta \in x, y, z$.

$$\overline{\overline{\mu_\alpha}} = \overline{\overline{\Psi}}^{\dagger} \frac{\overline{\overline{\hat{H}_{ZEE}\big|_{B_\alpha=1}}}}{\mu_B} \overline{\overline{\Psi}} \tag{2.2.41}$$

$$G_{\alpha,\beta} = 2 \sum_{u=\psi,\psi'} \sum_{v=\psi,\psi'} \mu_{\alpha_{u,v}} \mu_{\beta_{v,u}} \tag{2.2.42}$$

This g-tensor is then diagonalized to yield three principle values and their corresponding directions, leading to the definition of the anisotropic g-tensor for each pseudo-spin doublet. By convention, the directions are defined such that $g_x < g_y < g_z$.

Transition probabilities

For anisotropic systems, the zero-field average transition probability between states u and v is calculated through Equation 2.2.44, using the expectation values of the three Cartesian magnetic moment operators, Equation 2.2.41. The transition probabilities are in units of squared Bohr magnetons (${\mu_B}^2$).

$$T_{u,v} = \frac{1}{3} \sum_{\alpha=x,y,z} \left| \left\langle v \middle| \sum_{i=1}^{N} \left(\hat{H}_{ZEE}\big|_{B_\alpha=1} \right) \middle| u \right\rangle \right|^2 \tag{2.2.44}$$

J-mixing

For calculations on single lanthanide ions in the $|L_i, m_{L_i}, S_i, m_{S_i}\rangle$ basis, the wavefunction is expressed also in the $|J_i, m_{J_i}\rangle$ basis, though a Clebsch-Gordan decomposition. This provides a means of investigating the extent of *J*-mixing by the CF.

Non-collinearity

For single magnetic centres the orientation of the reference frame is always an arbitrary choice and any symmetry elements that may be identified, by crystallography or other means, can be related to this axis. When considering multiple magnetic sites in a single compound, while the global reference frame is still arbitrary, the individual reference frames, which may possess defined symmetry elements, may not be coincident and in which case it would not be ideal to enforce the global frame upon all sites. Therefore *PHI* allows users to rotate individual reference frames of the magnetic centres to allow for a description of each centre in its own, most convenient, reference frame. The two sources of magnetic anisotropy in *PHI* are the anisotropic g-tensor and the CF Hamiltonian. The diagonal g-tensor and/or the exchange matrix can be rotated into the local frame, using the Z-Y’-Z’’ convention according to Equations 2.2.45 – 2.2.49. The rotation of the CFPs is performed according to Mulak and Mulak’s convention,[32] with a slight modification. The rotation of a set of CFPs of a given rank, in Wybourne notation, is given by Equation 2.2.50, where the elements of the unitary rotation matrix, $\bar{\bar{D}}$, are given by Equation 2.2.51. The symbols in brackets in Equation 2.2.51 are binomial coefficients.

Note that *PHI* and *EasySpin* use very different conventions for rotation matrices, but by a happy coincidence the practical use of the three Euler angles is identical.

$$\overline{\overline{R_z}}(\theta) = \begin{matrix} \cos\theta & -\sin\theta & 0 \\ \sin\theta & \cos\theta & 0 \\ 0 & 0 & 1 \end{matrix} \tag{2.2.45}$$

$$\overline{\overline{R_y}}(\theta) = \begin{matrix} \cos\theta & 0 & \sin\theta \\ 0 & 1 & 0 \\ -\sin\theta & 0 & \cos\theta \end{matrix} \tag{2.2.46}$$

$$\overline{\overline{R^{PHI}}}(\alpha,\beta,\gamma) = R_z(\alpha)\cdot R_y(\beta)\cdot R_z(\gamma) \tag{2.2.47}$$

$$\overline{\overline{G'}} = \overline{\overline{R^{PHI}}}(\alpha,\beta,\gamma)\cdot \bar{\bar{G}}\cdot \overline{\overline{R^{PHI}}}^{T}(\alpha,\beta,\gamma) \tag{2.2.48}$$

$$\overline{\overline{J_{ij}}'} = \overline{\overline{R^{PHI}}}(\alpha,\beta,\gamma)\cdot \overline{\overline{J_{ij}}}\cdot \overline{\overline{R^{PHI}}}^{T}(\alpha,\beta,\gamma) \tag{2.2.49}$$

$$\overrightarrow{B'_k} = \bar{\bar{D}}^{(k)}(\alpha,\beta,\gamma)\cdot \overrightarrow{B_k} \tag{2.2.50}$$

$$D^{(k)}{}_{m,n}(\alpha,\beta,\gamma) = e^{i(m\alpha+n\gamma)}\sqrt{\frac{(k+m)!\,(k-m)!}{(k+n)!\,(k-n)!}}$$
$$\times\sum_{p=0}^{2k}\binom{k+n}{k-m-p}\binom{k-n}{p}(-1)^{k-m-p}cos\left(\frac{-\beta}{2}\right)^{2p+m+n}\quad sin\left(\frac{-\beta}{2}\right)^{2k-2p-m-n}$$
(2.2.51)

TIP, intermolecular interactions and magnetic impurities

A Temperature Independent Paramagnetic (TIP) component can be added to the calculated magnetic susceptibility, directly in units of cm^3 mol^{-1}, Equation 2.2.52.

Intermolecular interactions between spin systems can be modelled using the mean-field approximation, Equation 2.2.53; this expression changed as of version 2.0 to allow its use in anisotropic systems.

Magnetic impurities are included employing analytical expressions for the field and temperature dependent magnetization, magnetic susceptibility and heat capacity, assuming the impurities are pure spin centres with g = 2.0. As of version 2.0, the impurity value represents the fraction of the system, Equations 2.2.54 – 2.2.56.

These effects are included in the order of TIP, *zJ*, magnetic impurity, giving the final expression for the magnetic susceptibility, Equation 2.2.57.

$$\chi_{TIP} = \chi_{calc} + TIP \qquad (2.2.52)$$

where TIP is the temperature independent paramagnetism

$$\chi_{zJ} = \frac{\chi_{TIP}}{1-\left(\frac{zJ}{N_A{\mu_B}^2}\right)\chi_{TIP}} \qquad (2.2.53)$$

where zJ is the intermolecular interaction parameter

$$\chi = (1-IMP)\chi_{zJ} + (IMP)\chi_{IMP} \qquad (2.2.54)$$

$$M = (1-IMP)M_{calc} + (IMP)M_{IMP} \qquad (2.2.55)$$

$$C = (1-IMP)C_{calc} + (IMP)C_{IMP} \qquad (2.2.56)$$

where χ_{IMP} is the field and temperature dependent magnetic susceptibility of the impurity
M_{IMP} is the field and temperature dependent magnetization of the impurity
C_{IMP} is the field and temperature dependent heat capacity of the impurity
IMP is the fraction of magnetic impurity

$$\chi = (1 - IMP)\frac{\chi_{calc} + TIP}{1 - \left(\frac{zJ}{N_A {\mu_B}^2}\right)(\chi_{calc} + TIP)} + (IMP)\chi_{IMP} \qquad (2.2.57)$$

Electron Paramagnetic Resonance

The simulation of EPR spectra is not a simple task. Due to the field swept nature of the experiment, the action of the magnetic field on the sample must be accounted for and generally cannot be treated as a perturbation. Therefore, evaluation of the field dependent wavefunctions is required. Many approaches for this task have been employed, using various approximations, most of which involve searching the energy manifolds for transitions.[33,34] In *PHI*, the EPR spectrum is calculated *via* a ‘brute-force’ approach which considers the transition probability for every pair of states at each field point explicitly. While this approach is very computationally intensive, it does not rely on any approximations and includes all transitions, whether deemed to be ‘allowed’ or ‘forbidden’ as well as looping transitions. The EPR absorption as a function of field is calculated through Equation 2.2.58 or 2.2.59 for perpendicular or parallel mode, respectively.

There is also the possibility in *PHI* to calculate EPR spectra using infinite order perturbation theory. The structure of the code is almost identical to that for the full method, however in place of diagonalization of the full Hamiltonian, the exchange and Zeeman components are treated as perturbations to the zeroth order wavefunctions, which are the eigenfunctions of the SO and CF Hamiltonians. This method therefore assumes knowledge of the single-site properties for each ion, which can then be perturbed by the exchange interaction and magnetic field. Of course this is inappropriate in large magnetic fields or if the exchange interactions are stronger than the SO or CF terms.

The linewidth function assumes a pseudo-voigt profile (Equation 2.2.60),[35] which has shown to be required in certain applications.[36] The linewidth is treated in frequency space and therefore no frequency-field conversion factor (commonly referred to as the $\frac{1}{g}$ factor) is required.[37,38] Note that the x' and y' directions are determined as mutually orthogonal to the main magnetic field, $\vec{B}$, while the z' direction is parallel to it.

$$A(\vec{B}) = \sum_{i<j}^{i,j\in dim} \left(\left| \left\langle j \middle| \hat{H}_{ZEE}\Big|_{B_{\overrightarrow{x'}}=1} \middle| i \right\rangle \right|^2 + \left| \left\langle j \middle| \hat{H}_{ZEE}\Big|_{B_{\overrightarrow{y'}}=1} \middle| i \right\rangle \right|^2 \right) \frac{\left(e^{\frac{-E_i}{k_B T}} - e^{\frac{-E_j}{k_B T}} \right)}{Z} V(\Delta E, \eta_{ij}, v)$$

(2.2.58)

$$A(\vec{B}) = \sum_{i<j}^{i,j\in dim} \left| \left\langle j \middle| \hat{H}_{ZEE}\Big|_{B_{\overrightarrow{z'}}=1} \middle| i \right\rangle \right|^2 \frac{\left(e^{\frac{-E_i}{k_B T}} - e^{\frac{-E_j}{k_B T}} \right)}{Z} V(\Delta E, \eta_{ij}, v) \tag{2.2.59}$$

where $|i\rangle$ and $j\rangle$ are two eigenstates evaluated at $\vec{B}$
$\Delta E = \left| |E_i - E_j| - E_{MW} \right|$
η_{ij} is the linewidth
v is the voigt parameter

$$V(\Delta E, \eta, v) = v \frac{2}{\pi\eta\left(1 + 4\left(\frac{\Delta E}{\eta}\right)^2\right)} + (1 - v)\frac{2\sqrt{\ln 2}}{\sqrt{\pi}\eta e^{-4\ln 2\left(\frac{\Delta E}{\eta}\right)^2}} \tag{2.2.60}$$

As with the calculation of powder thermodynamic magnetic properties of anisotropic systems, the EPR absorption signal must be integrated over all possible orientations of the magnetic field; the ZCW scheme as discussed above is used for this purpose. After the absorption spectrum is calculated, it is normalized and if requested the first or second derivative or the integration is taken *via* finite differences.

The EPR linewidth can be anisotropic to account for unresolved spectral features such as hyperfine coupling. This is performed using the direction cosines for the direction of the external magnetic field, Equation 2.2.61.[36] The linewidth can also be augmented to include the effects of crystal mosacity,[39] and/or strain in the spin Hamiltonian parameters,[36] which is performed for each pair of states, Equation 2.2.62. These derivatives are evaluated analytically using the Hellmann-Feynman theorem.[40]

$$\eta_0 = \sqrt{\eta_x{}^2\left(\overrightarrow{z'}\cdot\vec{x}\right)^2 + \eta_y{}^2\left(\overrightarrow{z'}\cdot\vec{y}\right)^2 + \eta_z{}^2\left(\overrightarrow{z'}\cdot\vec{z}\right)^2} \tag{2.2.61}$$

$$\eta_{ij} = \sqrt{{\eta_0}^2 + \omega^2 \left(\left(\frac{\partial E_i}{\partial B_\theta} - \frac{\partial E_j}{\partial B_\theta} \right)^2 + \left(\frac{\partial E_i}{\partial B_\varphi} - \frac{\partial E_j}{\partial B_\varphi} \right)^2 \right) + \sum_p \left(\frac{\partial \left(E_j - E_i \right)}{\partial p} \right)^2 {\sigma_p}^2} \quad (2.2.62)$$

where ω is the mosacity parameter
p is a parameter of the spin Hamiltonian
σ_p is the strain in parameter p

Error residuals and Uncertainties

In all cases, the error for a particular data set is calculated following the sum of squares approach, Equation 2.2.63 as an example for magnetization and susceptibility. When calculating the total error for a simultaneous comparison to multiple data sets, the total residual is calculated as the product of the individual sum of squares errors for each data set. In this way, different error scales of the individual data sets will not obscure features in one dataset.

$$Res = \left[\sum_{i=1}^{points} \left(M_{exp} - M_{calc} \right)^2 \right] \left[\sum_{i=1}^{points} \left(\chi_{exp} - \chi_{calc} \right)^2 \right] \quad (2.2.63)$$

After parameters have been optimised to fit a particular model to an experimental data set, the uncertainties in the optimal parameters are reported. The hessian matrix (Equation 2.2.64) and the covariance matrix are calculated at the minimum (Equation 2.2.65).[41] The uncertainty for each free variable is the square root of the diagonal element of the covariance matrix (Equation 2.2.66), and the correlation between two parameters is given by Equation 2.2.67.

$$\bar{\bar{H}} = \begin{bmatrix} \frac{\partial^2 Res}{\partial {v_1}^2} & \frac{\partial^2 Res}{\partial v_1 \partial v_2} & \cdots & \frac{\partial^2 Res}{\partial v_1 \partial v_n} \\ \frac{\partial^2 Res}{\partial v_2 \partial v_1} & \frac{\partial^2 Res}{\partial {v_2}^2} & \cdots & \frac{\partial^2 Res}{\partial v_2 \partial v_n} \\ \vdots & \vdots & \ddots & \vdots \\ \frac{\partial^2 Res}{\partial v_n \partial v_1} & \frac{\partial^2 Res}{\partial v_n \partial v_2} & \cdots & \frac{\partial^2 Res}{\partial {v_n}^2} \end{bmatrix} \quad (2.2.64)$$

$$\bar{\bar{C}} = \frac{\bar{\bar{H}}^{-1} Res}{points - variables} \quad (2.2.65)$$

$$\sigma_i = \sqrt{\bar{\bar{C}}_{i,i}} \quad (2.2.66)$$

$$\rho_{i,j} = \frac{\bar{\bar{C}}_{i,j}}{\sigma_i \sigma_j} \quad (2.2.67)$$

3. Code Description

3.1 PHI

PHI is written in Fortran95 and C++. The GUI is written in C++ using the Qt toolkit and the Quantum Mechanics is written in Fortran95. The latter is split into six modules for easy maintenance; *data.f90*, *ang_mom.f90*, *powder.f90*, *props.f90*, *fitting.f90* and *phi.f90*.

data.f90 contains all the explicit variable declarations for global variables and arrays. It also contains a number of subroutines which initialize constants, read input files, write output files and perform diagnostics.

ang_mom.f90 contains all the Hamiltonian operators and tools required for matrix operations.

powder.f90 contains the routines required for powder integration procedures.

props.f90 contains the subroutines for the calculation of the magnetic properties.

fitting.f90 contains the subroutines necessary to perform surveys and fits, containing residual calculation routines and fitting algorithms.

phi.f90 is the main program which controls what calculations are to be performed.

The program can be well understood by means of an operational schematic, Figure 3.1.1.

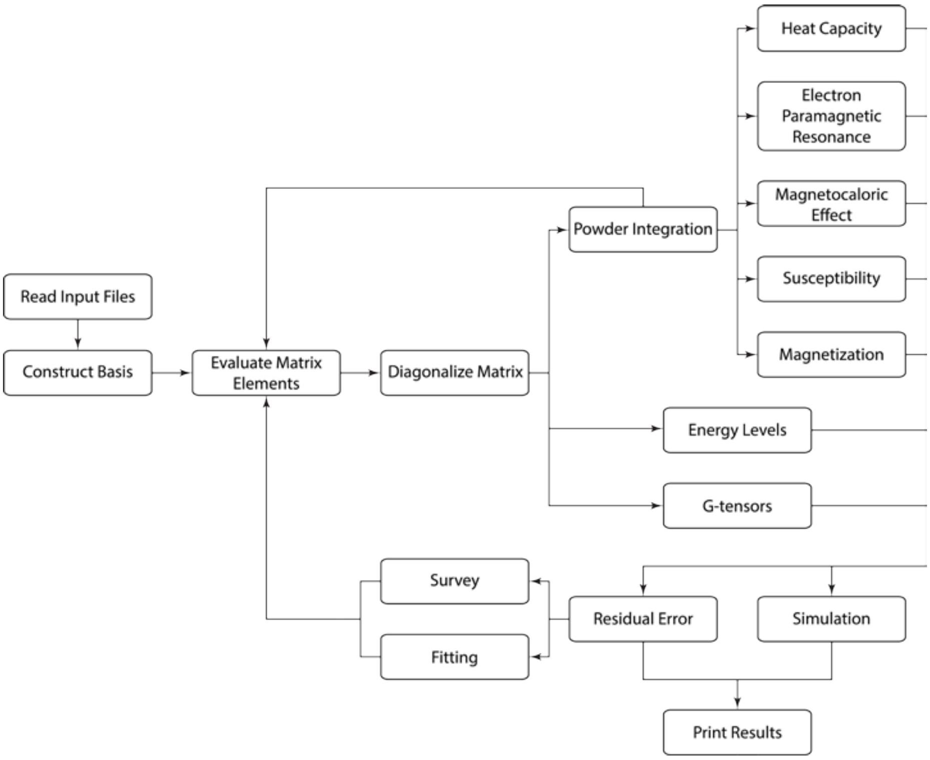

Figure 3.1.1 – Operational schematic of *PHI*

PHI has been written to take advantage of multiple processor cores, now common in consumer and specialized machines. There are two models of parallelism currently supported by *PHI* – Symmetric Multi-Processing (SMP) and Single Process Multiple Data (SPMD) – which use fundamentally different ideas to perform tasks more efficiently compared to a sequential model. The simplest approach to increase computational efficiency is to employ multiple cores on a shared memory machine (SMP model) to perform multiple diagonalizations simultaneously, which is achieved in *PHI* using OpenMP threads to distribute work. However, the SMP model is clearly limited by the size of the machine, both the number of cores and available memory. For this reason, the SPMD model is one of the most common parallel strategies due to the cost effectiveness of multiple smaller machines. *PHI* uses the MPI standard to distribute work amongst an arbitrary number of processes connected by a network.

Multi-dimensional non-linear optimization is a difficult problem, often requiring in-depth parameter space analysis to determine the global minimum for a given problem. For this reason, *PHI* contains two internal fitting algorithms, Powell's method[42] and the Simplex method,[43] which have been implemented based on those described in Numerical Recipes for Fortran.[44] The Simplex method is well suited to optimizing nearby minima while Powell's method is often useful in situations where a good initial guess is not available.

PHI contains several functions from the Fortran version of Stevenson's *anglib* library[45] – modified versions of the functions '*cleb*', '*sixj*', '*binom*' and '*angdelta*' are contained within the source.

Since version 3.0, *PHI* can be compiled with a GUI written in C++ with the Qt framework. The direct compilation of the GUI in this way means that data can be shared between the two codes, leading to better performance and tighter integration. In addition to the Qt GUI toolkit, *PHI* makes use of the QCustomPlot library[46] for plotting.

4. User Guide

4.1 Binaries and compilation

PHI is available as a command line binary, GUI binary or as source code.

To compile *PHI* from source, the Makefile must be tailored to the specifications of the system at hand, a Fortran95 compiler must be available and the appropriate libraries need to be compiled and in known locations. The source files ***must*** be listed in the order shown in the Makefile or errors will be encountered. *PHI* must be compiled using a C pre-processor, which provides a means for compiling different versions of the code from the same source files. Table 4.1.1 shows the compile time options. Even without SMP or SPMD activated, the C pre-processor must still be invoked. If compiling for SPMD, it is recommended to use your MPI library's wrapper compiler, eg "mpifort" with the additional libraries and options required by *PHI*. It is recommended that *PHI* be compiled with the highest level of compiler optimization and inter-procedural optimization. Note that the source code is written in free-form Fortran95 and therefore compilers such as gfortran need the '-ffree-line-length-3500' flag (or similar). The supplied Makefile provides a skeleton to set up a custom compilation of *PHI*. The variables at the top of the file must be set in order to compile the program. COMPILER is your Fortran 95 compiler, e.g. ifort or gfortran. MPI_COMPILER is your wrapper MPI compiler, e.g. mpifort. FLAGS and MPI_FLAGS can be adjusted as the user pleases. LAPACK must be set to the appropriate library destination and contain links to lapack and blas. SOURCES is the list of source files for *PHI* and must be in the default order. The flags in the Makefile may be specific to the ifort compiler and therefore must be substituted for their equivalent flag for your compiler (e.g. -openmp becomes -fopenmp for gfortran).

For compilation of the GUI version, we recommended using the Qt creator software with the PHI.pro.user files provided as a guide. Note that the appropriate compilers and linear algebra libraries will be required in this case also.

Table 4.1.1 – Compile time options

Option	C pre-processor flag	Other required flags	Additional libraries	Forbidden flags
SMP (OpenMP)	-Domp	-openmp		-Dmpi
SPMD (MPI)	-Dmpi		MPI	-Domp
GUI	-Dgui			

4.2 Program execution

To run *PHI* on the command line, it is as simple as launching the executable on the command line from the working directory containing the input file, e.g. “phi_vx.x_linux64.x test-job”, where test-job is the name of the input file.

The GUI version is launched by simply running PHI.exe on Windows, PHI.app on MacOS or PHI.sh on LINUX.

4.3 Input files and syntax

Input to the program is via plain text input and data files. The job name used to launch the program (Section 4.2) defines the name of the associated input and data files *PHI* will look for. It will look for files in the directory that the program was launched from, the current working directory. For the above example, *PHI* will look for “test-job.input” in the current directory. This input file contains all the instructions that *PHI* needs to perform calculations. The other data files required vary based on the type of calculation specified by the input file. A total list of input and data files is given below, using the example job name.

test-job.input	Contains all input specifications and parameters
test-job_mag.exp	Contains experimental magnetization data
test-job_sus.exp	Contains experimental susceptibility data
test-job_tensor.exp	Contains experimental magnetic susceptibility tensor data
test-job_levels.exp	Contains experimental energy levels
test-job_G.exp	Contains experimental g-tensors
test-job_mce.exp	Contains experimental MCE data
test-job_epr.exp	Contains experimental EPR data
test-job_heat.exp	Contains experimental heat capacity data

.input specification

This file is delimited into blocks by headers, signified by four asterisks, “****”. The first block ***must be*** the ****Spin ***or*** ****Ion block (see below) and the input file ***must be*** terminated by “****End”. The input file is not case-sensitive, despite the notation given in this manual for clarity. After the “****End” termination line, the input file is not read by *PHI* and so may contain descriptions, other input specifications or comments. Also, any line that begins with ! or # or / is interpreted as a comment and not read by *PHI*.

The first block, which must be the ****Spin ***or*** ****Ion block, specifies the number and type of magnetic centres in the problem and this can be done in ***one of two ways***.

Method 1:

*****Spin block*

In the first method, the ‘full’ input method, the first line ***must be*** “****Spin” and the subsequent lines denote the spin angular momentum of the centres. The ‘spins’ are entered as two times the spin ($2S_i$), or the number of unpaired electrons. Note that these spins may be real spins or pseudo-spins. In the following example, three paramagnetic centres are declared with spins $S_1 = 2, S_2 = S_3 = S_4 = 5/2$.

```
****Spin
4
5
5
5
```

*****Orbit block*

In the ‘full’ input method, the “****Orbit” block is also used, which details the corresponding orbital angular momentum of each site declared in the ****Spin block. Like the ****Spin block, the orbital moments must be entered as two times the orbital moment ($2L_i$). If this block is omitted, the orbital moments are all assumed to be zero. This example assigns $L_1 = L_2 = L_3 = 0$ and $L_4 = 5$, corresponding to the spins above.

```
****Orbit
0
0
0
10
```

Method 2:

*****Ion block*

The above two blocks can be efficiently replaced in the case of common situations, by using the ‘simple’ input method. To use the simple input method, the first line ***must be*** “****Ion” and the subsequent lines define the centres in a standard notation. The example below would make exactly the same assignments as specified in the examples above, under certain assumptions.

```
****Ion
Mn(III)Oh(w)
Fe(III)Oh(w)
Fe(III)Oh(w)
Dy(LS)
```

The possible keywords for the ****Ion block are given in Table 4.3.1 with the specifications that they designate. Since version 3.0, nuclear spins for elements with a single isotope comprising > 90% natural abundance can be included using the ****Ion block. Note that the Hamiltonian conventions given in section 2.2 still apply.

Table 4.3.1 – Ion types

Keyword	**Term**	**S**	**L**	**λ (cm^{-1})**	**σ**	**Comment**
Ee	^2S	1/2	0	-	-	Radical
Ti(III)Oh	$^2T_{2g}$	1/2	1	155.0	-1.0	O_h symmetry
Ti(III)Td	^2E	1/2	0	-	-	T_d symmetry
Ti(III)FI	^2D	1/2	2	155.0	1.0	Spherical symmetry
Ti(II)Oh	$^3T_{1g}$	1	1	61.5	-1.5	O_h symmetry
Ti(II)Td	$^3A_2$	1	0	-	-	T_d symmetry
Ti(II)FI	^3F	1	3	61.5	1.0	Spherical symmetry
V(IV)Oh	$^2T_{2g}$	1/2	1	250.0	-1.0	O_h symmetry
V(IV)Td	^2E	1/2	0	-	-	T_d symmetry
V(IV)FI	^2D	1/2	2	250.0	1.0	Spherical symmetry
V(III)Oh	$^3T_{1g}$	1	1	105.0	-1.5	O_h symmetry
V(III)Td	$^3A_2$	1	0	-	-	T_d symmetry
V(III)FI	^3F	1	3	105.0	1.0	Spherical symmetry
V(II)Oh	$^4A_{2g}$	3/2	0	-	-	O_h symmetry
V(II)Td(w)	$^4T_1$	3/2	1	56.5	-1.5	T_d symmetry, weak CF
V(II)Td(s)	^2E	1/2	0	-	-	T_d symmetry, strong CF
V(II)FI	^4F	3/2	3	56.5	1.0	Spherical symmetry
Cr(III)Oh	$^4A_{2g}$	3/2	0	-	-	O_h symmetry
Cr(III)Td(w)	$^4T_1$	3/2	1	91.5	-1.5	T_d symmetry, weak CF
Cr(III)Td(s)	^2E	1/2	0	-	-	T_d symmetry, strong CF
Cr(III)FI	^4F	3/2	3	91.5	1.0	Spherical symmetry
Cr(II)Oh(w)	^5E_g	2	0	-	-	O_h symmetry, weak CF
Cr(II)Td(w)	$^5T_2$	2	1	57.5	-1.0	T_d symmetry, weak CF
Cr(II)FI	^5D	2	2	57.5	1.0	Spherical symmetry
Mn(VI)Oh	$^2T_{2g}$	1/2	1	540.0	-1.0	O_h symmetry
Mn(VI)Td	^2E	1/2	0	-	-	T_d symmetry
Mn(VI)FI	^2D	1/2	2	540.0	1.0	Spherical symmetry
Mn(IV)Oh	$^4A_{2g}$	3/2	0	-	-	O_h symmetry
Mn(IV)Td(w)	$^4T_1$	3/2	1	138.5	-1.5	T_d symmetry, weak CF
Mn(IV)Td(s)	^2E	1/2	0	-	-	T_d symmetry, strong CF
Mn(IV)FI	^4F	3/2	3	138.5	1.0	Spherical symmetry
Mn(III)Oh(w)	^5E_g	2	0	-	-	O_h symmetry, weak CF
Mn(III)Td(w)	$^5T_2$	2	1	89.0	-1.0	T_d symmetry, weak CF
Mn(III)FI	^5D	2	2	89.0	1.0	Spherical symmetry
Mn(II)Oh(w)	$^6A_{1g}$	5/2	0	-	-	O_h symmetry, weak CF
Mn(II)Oh(s)	$^2T_{2g}$	1/2	1	-300.0	-1.0	O_h symmetry, strong CF

Mn(II)Td(w)	$^6A_1$	5/2	0	-	-	T_d symmetry, weak CF
Mn(II)FI	^6S	5/2	0	-	-	Spherical symmetry
Fe(VI)Oh	$^3T_{1g}$	1	1	332.5	-1.5	O_h symmetry
Fe(VI)Td	$^3A_2$	1	0	-	-	T_d symmetry
Fe(VI)FI	^3F	1	3	332.5	1.0	Spherical symmetry
Fe(III)Oh(w)	$^6A_{1g}$	5/2	0	-	-	O_h symmetry, weak CF
Fe(III)Oh(s)	$^2T_{2g}$	1/2	1	-460.0	-1.0	O_h symmetry, strong CF
Fe(III)Td(w)	$^6A_1$	5/2	0	-	-	T_d symmetry, weak CF
Fe(III)FI	^6S	5/2	0	-	-	Spherical symmetry
Fe(II)Oh(w)	$^5T_{2g}$	2	1	-100.0	-1.0	O_h symmetry, weak CF
Fe(II)Td(w)	^5E	2	0	-	-	T_d symmetry, weak CF
Fe(II)FI	^5D	2	2	-100.0	1.0	Spherical symmetry
Co(III)Oh(w)	$^5T_{2g}$	2	1	-145.0	-1.0	O_h symmetry, weak CF
Co(III)Td(w)	^5E	2	0	-	-	T_d symmetry, weak CF
Co(III)FI	^5D	2	2	-145.0	1.0	Spherical symmetry
Co(II)Oh(w)	$^4T_{1g}$	3/2	1	-171.5	-1.5	O_h symmetry, weak CF
Co(II)Oh(s)	^2E_g	1/2	0	-	-	O_h symmetry, strong CF
Co(II)Td	$^4A_2$	3/2	0	-	-	T_d symmetry
Co(II)FI	^4F	3/2	3	-171.5	1.0	Spherical symmetry
Ni(III)Oh(w)	$^4T_{1g}$	3/2	1	-235.0	-1.5	O_h symmetry, weak CF
Ni(III)Oh(s)	^2E_g	1/2	0	-	-	O_h symmetry, strong CF
Ni(III)Td	$^4A_2$	3/2	0	-	-	T_d symmetry
Ni(III)FI	^4F	3/2	3	-235.0	1.0	Spherical symmetry
Ni(II)Oh	$^3A_{2g}$	1	0	-	-	O_h symmetry
Ni(II)Td	$^3T_1$	1	1	-315.0	-1.5	T_d symmetry
Ni(II)FI	^3F	1	3	-315.0	1.0	Spherical symmetry
Cu(II)Oh	^2E_g	1/2	0	-	-	O_h symmetry
Cu(II)Td	$^2T_2$	1/2	1	-830.0	-1.0	T_d symmetry
Cu(II)FI	^2D	1/2	2	-830.0	1.0	Spherical symmetry
Ce(J)	$^2F_{5/2}$	5/2	0	-	-	Spherical symmetry
Ce(LS)	^2F	1/2	3	Table 2.2.1	1.0	Spherical symmetry
Pr(J)	$^3H_4$	4	0	-	-	Spherical symmetry
Pr(LS)	^3H	1	5	Table 2.2.1	1.0	Spherical symmetry
Nd(J)	$^4I_{9/2}$	9/2	0	-	-	Spherical symmetry
Nd(LS)	^4I	3/2	6	Table 2.2.1	1.0	Spherical symmetry
Pm(J)	$^5I_4$	4	0	-	-	Spherical symmetry
Pm(LS)	^5I	2	6	Table 2.2.1	1.0	Spherical symmetry
Sm(J)	$^6H_{5/2}$	5/2	0	-	-	Spherical symmetry
Sm(LS)	^6H	5/2	5	Table 2.2.1	1.0	Spherical symmetry
Eu(LS)	^7F	3	3	Table 2.2.1	1.0	Spherical symmetry
Gd(III)	^8S	7/2	0	-	-	Spherical symmetry

Tb(J)	$^7F_6$	6	0	-	-	Spherical symmetry
Tb(LS)	^7F	3	3	Table 2.2.1	1.0	Spherical symmetry
Dy(J)	$^6H_{15/2}$	15/2	0	-	-	Spherical symmetry
Dy(LS)	^6H	5/2	5	Table 2.2.1	1.0	Spherical symmetry
Ho(J)	$^5I_8$	8	0	-	-	Spherical symmetry
Ho(LS)	^5I	2	6	Table 2.2.1	1.0	Spherical symmetry
Er(J)	$^4I_{15/2}$	15/2	0	-	-	Spherical symmetry
Er(LS)	^4I	3/2	6	Table 2.2.1	1.0	Spherical symmetry
Tm(J)	$^3H_6$	6	0	-	-	Spherical symmetry
Tm(LS)	^3H	1	5	Table 2.2.1	1.0	Spherical symmetry
Yb(J)	$^2F_{7/2}$	7/2	0	-	-	Spherical symmetry
Yb(LS)	^2F	1/2	3	Table 2.2.1	1.0	Spherical symmetry
1H	-	1/2	0	-	-	$g_{\mathrm{eff}} = -3.04206422539567\times10^{-3}$
7Li	-	3/2	0	-	-	$g_{\mathrm{eff}} = 1.18233679972407\times10^{-3}$
9Be	-	3/2	0	-	-	$g_{\mathrm{eff}} = 4.27497106541515\times10^{-4}$
14N	-	1	0	-	-	$g_{\mathrm{eff}} = -2.19895100623363\times10^{-4}$
19F	-	1/2	0	-	-	$g_{\mathrm{eff}} = -2.86345235614900\times10^{-3}$
23Na	-	3/2	0	-	-	$g_{\mathrm{eff}} = -8.05133438386439\times10^{-4}$
27Al	-	5/2	0	-	-	$g_{\mathrm{eff}} = -7.93290633008815\times10^{-4}$
31P	-	1/2	0	-	-	$g_{\mathrm{eff}} = -1.23257717246290\times10^{-3}$
39K	-	3/2	0	-	-	$g_{\mathrm{eff}} = -1.42134142130333\times10^{-4}$
45Sc	-	7/2	0	-	-	$g_{\mathrm{eff}} = -7.40129043657371\times10^{-4}$
51V	-	7/2	0	-	-	$g_{\mathrm{eff}} = -8.01164269761082\times10^{-4}$
55Mn	-	5/2	0	-	-	$g_{\mathrm{eff}} = -7.52279448711121\times10^{-4}$
59Co	-	7/2	0	-	-	$g_{\mathrm{eff}} = -7.19983661185914\times10^{-4}$
75As	-	3/2	0	-	-	$g_{\mathrm{eff}} = -5.22641694748156\times10^{-4}$
89Y	-	1/2	0	-	-	$g_{\mathrm{eff}} = 1.49677523139677\times10^{-4}$
93Nb	-	9/2	0	-	-	$g_{\mathrm{eff}} = -7.46778817109020\times10^{-4}$
103Rh	-	1/2	0	-	-	$g_{\mathrm{eff}} = 9.62882838862856\times10^{-5}$
115In	-	9/2	0	-	-	$g_{\mathrm{eff}} = -6.70586900165064\times10^{-4}$
127I	-	5/2	0	-	-	$g_{\mathrm{eff}} = -6.12862945362421\times10^{-4}$
133Cs	-	7/2	0	-	-	$g_{\mathrm{eff}} = -4.01775608553100\times10^{-4}$
139La	-	7/2	0	-	-	$g_{\mathrm{eff}} = -4.33055467544589\times10^{-4}$
141Pr	-	5/2	0	-	-	$g_{\mathrm{eff}} = -9.31403976823108\times10^{-4}$
159Tb	-	3/2	0	-	-	$g_{\mathrm{eff}} = -7.31420617982361\times10^{-4}$
165Ho	-	7/2	0	-	-	$g_{\mathrm{eff}} = -9.08421139832151\times10^{-4}$
169Tm	-	1/2	0	-	-	$g_{\mathrm{eff}} = 2.51613049521855\times10^{-4}$
175Lu	-	7/2	0	-	-	$g_{\mathrm{eff}} = -3.47356716417833\times10^{-4}$
181Ta	-	7/2	0	-	-	$g_{\mathrm{eff}} = -3.68863641365058\times10^{-4}$
197Au	-	3/2	0	-	-	$g_{\mathrm{eff}} = -5.29171652461937\times10^{-5}$
209Bi	-	9/2	0	-	-	$g_{\mathrm{eff}} = -4.97453158946455\times10^{-4}$

Note that for all d block ions and LS type f-block ions, the isotropic electronic spin g-factor is set to 2.0. For J type lanthanides, the isotropic g-factor is set to the appropriate g_J value.[17] For the d-block free-ions (FI) and LS type f-block ions, the appropriate operator equivalent factors are automatically included.

Other blocks

*****Gfactors block*

To specify the spin g-factors for the centres, the "****Gfactors" block is used. Unless specified, all g-factors are taken to be 2.0 by default. The syntax requires the site index followed by one ***or*** three values, indicating either an isotropic or anisotropic spin g-factor (g_x, g_y, g_z). Strain in the g-values for EPR simulations can be given independently for each component, in brackets immediately following the value. In the following example, the second centre is given an anisotropic spin g-factor of $g_x = g_y = 1.9$ and $g_z = 2.2$, where the g_z value has g-strain of 0.5, the third centre is also given an anisotropic spin g-factor of $g_x = 0.1$, $g_y = 2.5$ and $g_z = 11.9$ and the fourth centre is given an isotropic spin g-factor of 1.98.

```
****Gfactors
2 1.9 1.9   2.2(0.5)
3 0.1 2.5   11.9
4 1.98
```

*****Exchange block*

To define (an)isotropic exchange coupling interactions between the centres, the "****Exchange" block is used. The interactions are all zero by default, so only the required interactions should be listed. This is done on one line by specifying the index of the first site, followed by the index of the second site, followed by the isotropic or anisotropic exchange values in cm^{-1}. Only one ***or*** three values should be given, indicating either an isotropic exchange or the three diagonal components of the exchange matrix J_{xx}, J_{yy} and J_{zz}. Strain in the exchange parameters for EPR simulations is given in brackets immediately following the value. The following example specifies three coupling pathways between sites 1 and 2, 2 and 3 and 1 and 3, where the exchange involving site 1 is axially anisotropic and there is J-strain in the exchange between sites 2 and 3.

```
****Exchange
1     2     2.0 2.0 -6.0
2     3     5.5(1)
1     3     1.0 1.0 5.0
```

*****Antisymmetric block*

To define the antisymmetric components of exchange interactions between centres, the "****Antisymmetric" block is used. The interactions are all zero by default, so only the required interactions should be listed. This is done on one line by specifying the index of the first site, followed by the index of the second site, followed by the three components of the antisymmetric exchange in cm^{-1}. Strain in the antisymmetric exchange parameters for EPR simulations is given in brackets immediately following the value. The following example specifies antisymmetric exchange between sites 2 and 3. Note that handedness is preserved with *PHI*, so that switching the order of the interacting pair is equivalent to negating the antisymmetric exchange vector.

```
****Antisymmetric
2     3     0.1 -0.1 1.5
```

*****Interaction block*

To define completely asymmetric exchange interactions between centres, the "****Interaction" block is used. The interactions are all zero by default, so only the required interactions should be listed. The syntax is similar to that for the "****Fit" and "****Survey" blocks, see below. The first line for each exchange pair gives the site indices, followed by three lines for each row of the interaction tensor in cm^{-1}. The final line ***must be*** "----" which signifies the end of the interaction tensor. Strain in the interaction tensor for EPR simulations is given in brackets immediately following the value. Note that handedness is preserved with *PHI*, so that switching the order of the interacting pair will imply usage of the transpose of the given exchange tensor.

```
****Interaction
2     3
Jxx Jxy Jxz
Jyx Jyy Jyz
Jzx Jzy Jzz
----
```

*****SOCoupling block*

To define or modify the SO Coupling parameters, the "****SOCoupling" block is used. The syntax requires the site index followed by up to six values representing the first to sixth order SO Coupling parameters in cm^{-1}. Strain in the SO parameters for EPR simulations is given in brackets immediately following the value. This example sets the parameters for the sites 1 and 5 only, where site 5 has only a first order component, while site 1 has both first and second order, where the second order component has some strain.

```
****SOCoupling
1     421.0 -5.78(0.2)
5     -165.0
```

*****OReduction block*

The combined orbital reduction parameters can be set, through the use of this block. These are specified by the index of the site followed by the value of the total orbital reduction parameter. A value of 1.0 removes the feature (default), i.e. no orbital reduction. Strain in the orbital reduction parameters for EPR simulations is given in brackets immediately following the value. In this example, site 5 is given a total orbital reduction parameter of 0.98 (be sure not to confuse the terminology and sign of the parameter when using the T,P equivalence method[19]).

```
****OReduction
5     0.98
```

*****CrystalField block*

A CF may be specified by using the “****CrystalField” block. The syntax requires the site index, followed by the rank, order and then value of the parameter in cm^{-1}. The site index, rank and order must be integers, while the CFPs must be real numbers. If the ‘full’ input method was used, operator equivalent factors are ***not*** included by *PHI* automatically and they must be included in the input parameters explicitly, if required. However if the ‘simple’ input method was used, the operator equivalent factors for the lanthanides and d-block free-ions are automatically included by *PHI*. Strain in the CF parameters for EPR simulations is given in brackets immediately following the value. The following example assumes the ****Spin block was used and therefore specifies the $B_2^0\theta_2$ parameter equal to -0.1 cm^{-1} for site 1 with a strain of 0.06 cm^{-1}, the $B_6^3\theta_6$ parameter equal to 0.0006 cm^{-1} for site 2 and the $B_4^{-1}\theta_4$ parameter equal to 0.230 cm^{-1}.

To describe a weak cubic field for the d-block free-ions, it is recommended to use the ‘Cubic N’ parameter (see Table 4.3.3). As the operator equivalent factors are taken into account using the simple input method, octahedral fields are described in all cases with a positive B_4^0 parameter and tetrahedral fields with a negative B_4^0 parameter.

Note the convention given in section 2.2 when using the $B_2^0\theta_2$ to represent the common ZFS parameter D, and the switch “ZFS I J K …” in the ****Params block.

```
****Crystal Field
1     2     0     -0.1(0.06)
2     6     3     0.0006
3     4     -1    0.230
```

*****Sus block*

This block provides all the options for the calculation of magnetic susceptibility. Table 4.3.2 gives all the available options for this block.

Table 4.3.2 – ****Sus block options

Parameter	Options/Syntax	Comments
Magnetic field direction / integration	Field STR Field Powder N Field Axial N Field Vector X Y Z	Selection of magnetic field: STR is either x, y or z for single directions or xyz for principal axes integration. If STR is ‘Powder’ then ZCW integration is used where N ≥ 0. If STR is Axial then integration with N points in the positive quadrant of the z-x plane is performed. If STR is ‘Vector’ an arbitrary single direction is given. If STR is ‘Angles’ an arbitrary single direction is given in polar

	Field Angles θ φ	coordinates in degrees. Default = “Field z” (isotropic), “Field xyz” (anisotropic).
Magnetic field	BSus A B C D …	Selects the magnetic field(s) in Tesla for the calculation. Any number of fields can be listed on the same line. Default = “BSus 0.01”.
Temperature sweep	Sweep Low High N <log>	Sets the temperature range (in Kelvin), the number of points and optionally spacing on a logarithmic scale. Default = “Sweep 1.8 300 250”.
Temperature Independent Paramagnetism	TIP X	Sets a TIP (in cm^3 mol^{-1}). Default = “TIP 0”.
Intermolecular interaction	zJ X	Sets the mean-field zJ parameter (in cm^{-1}). Default = “zJ 0”.
Differential susceptibility	Differential	Calculates the true differential susceptibility, as opposed to the default $\chi = M/B$.

*****Tensor block*

This block provides all the options for the calculation of the magnetic susceptibility tensor. Table 4.3.3 gives all the available options for this block.

Table 4.3.3 – ****Tensor block options

Parameter	**Options/Syntax**	**Comments**
Magnetic field	BSus A B C D …	Selects the magnetic field(s) in Tesla for the calculation. Any number of fields can be listed on the same line. Default = “BSus 0.01”.
Temperature sweep	Sweep Low High N <log>	Sets the temperature range (in Kelvin), the number of points and optionally spacing on a logarithmic scale. Default = “Sweep 1.8 300 250”.

*****Mag block*

This block provides all the options for the calculation of magnetization. Table 4.3.4 gives all the available options for this block.

Table 4.3.4 – ****Mag block options

Parameter	**Options/Syntax**	**Comments**
Magnetic field direction / integration	Field STR Field Powder N Field Axial N Field Vector X Y Z	Selection of magnetic field: STR is either x, y or z for single directions or xyz for principal axes integration. If STR is ‘Powder’ then ZCW integration is used where N ≥ 0. If STR is Axial then integration with N points in the positive quadrant of the z-x plane is performed. If STR is ‘Vector’ an arbitrary single direction is given. If STR is ‘Angles’ an arbitrary single direction is given in polar

	Field Angles θ φ	coordinates in degrees. Default = “Field z” (isotropic), “Field Powder 3” (anisotropic).
Temperature	TMag A B C D …	Selects the temperature(s) in Kelvin for the calculation. Any number of temperatures can be listed on the same line. Default = “TMag 2 4 10 20”.
Magnetic field sweep	Sweep Low High N <log>	Sets the magnetic field range (in Tesla), the number of points and optionally spacing on a logarithmic scale. Default = “Sweep 0 7 10”.

*****MCE block*

This block provides all the options for the calculation of the magnetocaloric effect. Table 4.3.5 gives all the available options for this block.

Table 4.3.5 – ****MCE block options

Parameter	**Options/Syntax**	**Comments**
Magnetic field direction / integration	Field STR Field Powder N Field Axial N Field Vector X Y Z Field Angles θ φ	Selection of magnetic field: STR is either x, y or z for single directions or xyz for principal axes integration. If STR is ‘Powder’ then ZCW integration is used where $N \geq 0$. If STR is Axial then integration with N points in the positive quadrant of the z-x plane is performed. If STR is ‘Vector’ an arbitrary single direction is given. If STR is ‘Angles’ an arbitrary single direction is given in polar coordinates in degrees. Default = “Field z” (isotropic), “Field Powder 3” (anisotropic).
Magnetic field	BMCE A B C D …	Selects the magnetic field(s) in Tesla for the calculation. Any number of fields can be listed on the same line. Default = “BMCE 7”.
Temperature sweep	Sweep Low High N <log>	Sets the temperature range (in Kelvin), the number of points and optionally spacing on a logarithmic scale. Default = “Sweep 1.8 50 250”.
Molecular mass	Mass X	Sets the molecular mass for the sample in g mol^{-1}. Default = “Mass 2000”.
Integration	Integrate N	Sets the number of magnetic field integration points. Default = “Integrate 50”.

*****HeatCapacity block*

This block provides all the options for the calculation of the heat capacity. Table 4.3.6 gives all the available options for this block.

Table 4.3.6 – ****HeatCapacity block options

Parameter	**Options/Syntax**	**Comments**
Magnetic field direction / integration	Field STR Field Powder N Field Axial N Field Vector X Y Z Field Angles θ φ	Selection of magnetic field: STR is either x, y or z for single directions or xyz for principal axes integration. If STR is 'Powder' then ZCW integration is used where N ≥ 0. If STR is Axial then integration with N points in the positive quadrant of the z-x plane is performed. If STR is 'Vector' an arbitrary single direction is given. If STR is 'Angles' an arbitrary single direction is given in polar coordinates in degrees. Default = "Field z" (isotropic), "Field Powder 3" (anisotropic).
Magnetic field	BHeat A B C D …	Selects the magnetic field(s) in Tesla for the calculation. Any number of fields can be listed on the same line. Default = "BHeat 0.1".
Temperature sweep	Sweep Low High N <log>	Sets the temperature range (in Kelvin), the number of points and optionally spacing on a logarithmic scale. Temperatures are on a base-10 logarithmic scale. Default = "Sweep 0.5 20 250 log".
Debye lattice contribution	Debye T_D α	Sets the Debye temperature (in Kelvin) and exponent. Default = "Debye 0 0"

*****EPR block*

The "****EPR" block is used to specify the options for the EPR calculation. The possible keywords are given in Table 4.3.7.

Table 4.3.7 – ****EPR block options

Parameter	**Options/Syntax**	**Comments**
Magnetic field direction / integration	Field STR Field Powder N Field Axial N Field Vector X Y Z Field Angles θ φ	Selection of magnetic field: STR is either x, y or z for single directions or xyz for principal axes integration. If STR is 'Powder' then ZCW integration is used where N ≥ 0. If STR is Axial then integration with N points in the positive quadrant of the z-x plane is performed. If STR is 'Vector' an arbitrary single direction is given. If STR is 'Angles' an arbitrary single direction is given in polar coordinates in degrees. Default = "Field Powder 6".

Temperature	TEPR A B C D …	Sets the temperature(s) for the simulation, in Kelvin. Default = “TEPR 5”.
Frequency	FEPR A B C D …	Sets the frequency(ies) for the simulation, in GHz. Default = “FEPR 9.5 35 94”.
Spectrum type	Type A B C D …	Selects whether the absorption (N = 0), first derivative (N = 1), second derivative (N = 2) or integrated absorption (N = -1) spectrum is to be calculated, for each frequency. Default = “Type 1 1 1 1 …”.
Parallel mode	Parallel	Selects parallel mode. Default = Off.
Magnetic field sweep	Sweep Low High N <log>	Sets the magnetic field range (in Tesla), the number of points and optionally spacing on a logarithmic scale. Default = “Sweep 0 1.6 250”.
Linewidth	LW A B C D …	Sets the isotropic pseudo-voigt linewidth, in GHz, for each frequency. If only one linewidth is given and multiple frequencies are to be simulated, then all frequencies have the same linewidth. Default = “Linewidth 0.27”.
Anisotropic linewidth, x-direction	LWX A B C D …	Sets the anisotropic pseudo-voigt linewidth for the x-direction, in GHz, for each frequency. If only one linewidth is given and multiple frequencies are to be simulated, then all frequencies have the same linewidth. Default = “Linewidth 0.27”.
Anisotropic linewidth, y-direction	LWY A B C D …	Sets the anisotropic pseudo-voigt linewidth for the y-direction, in GHz, for each frequency. If only one linewidth is given and multiple frequencies are to be simulated, then all frequencies have the same linewidth. Default = “Linewidth 0.27”.
Anisotropic linewidth, z-direction	LWZ A B C D …	Sets the anisotropic pseudo-voigt linewidth for the z-direction, in GHz, for each frequency. If only one linewidth is given and multiple frequencies are to be simulated, then all frequencies have the same linewidth. Default = “Linewidth 0.27”.
Pseudo-voigt parameter	Voigt A B C D …	Sets the pseudo-voigt parameter for each frequency. If only one parameter is given and multiple frequencies are to be simulated, then all frequencies have the same parameter. Default = “Voigt 1” (Lorentzian).
Mosaicity	Mosaic A B C D …	Sets the mosacity parameter for each frequency. If only one parameter is given and multiple frequencies are to be simulated, then all frequencies have the same parameter.

		Default = “Mosaic 0”.
Absolute intensity	NoNorm	Gives the calculated EPR data in absolute intensity units without normalization.
Infinite order perturbation theory	Subspace N	Uses subspace perturbation theory to calculate the EPR spectrum for the N lowest lying states. Default = Off

*****Zeeman block*

The “****Zeeman” block is used to specify the options for the Zeeman calculation. The possible keywords are given in Table 4.3.8.

Table 4.3.8 – Zeeman options

Parameter	**Options/Syntax**	**Comments**
Magnetic field direction	Field STR Field Vector X Y Z Field Angles θ φ	Selection of magnetic field: STR is either x, y or z for single directions or xyz for principal axes integration. If STR is ‘Vector’ an arbitrary single direction is given. If STR is ‘Angles’ an arbitrary single direction is given in polar coordinates in degrees. Default = “Field z”.
Magnetic field sweep	Sweep Low High N <log>	Sets the magnetic field range (in Tesla), the number of points and optionally spacing on a logarithmic scale. Default = “Sweep 0 7 250”.

Either the full calculation or the approximation scheme (in cases where applicable) may be used to perform such a sweep. If using the full calculation method, please note that due to the convention of matrix diagonalization routines, the eigenvalues are returned in ascending order, thus presenting artefacts at level crossings which appear like avoided crossings. This is demonstrated in Figure 4.3.1 with a simple isotropic case using the full calculation (top) and the approximation method (bottom), both with 10 steps. It is clearly seen that the level crossings are not correctly displayed in the top figure due to the width of the steps and the eigenvalue re-ordering. This can be corrected visually by increasing the number of steps.

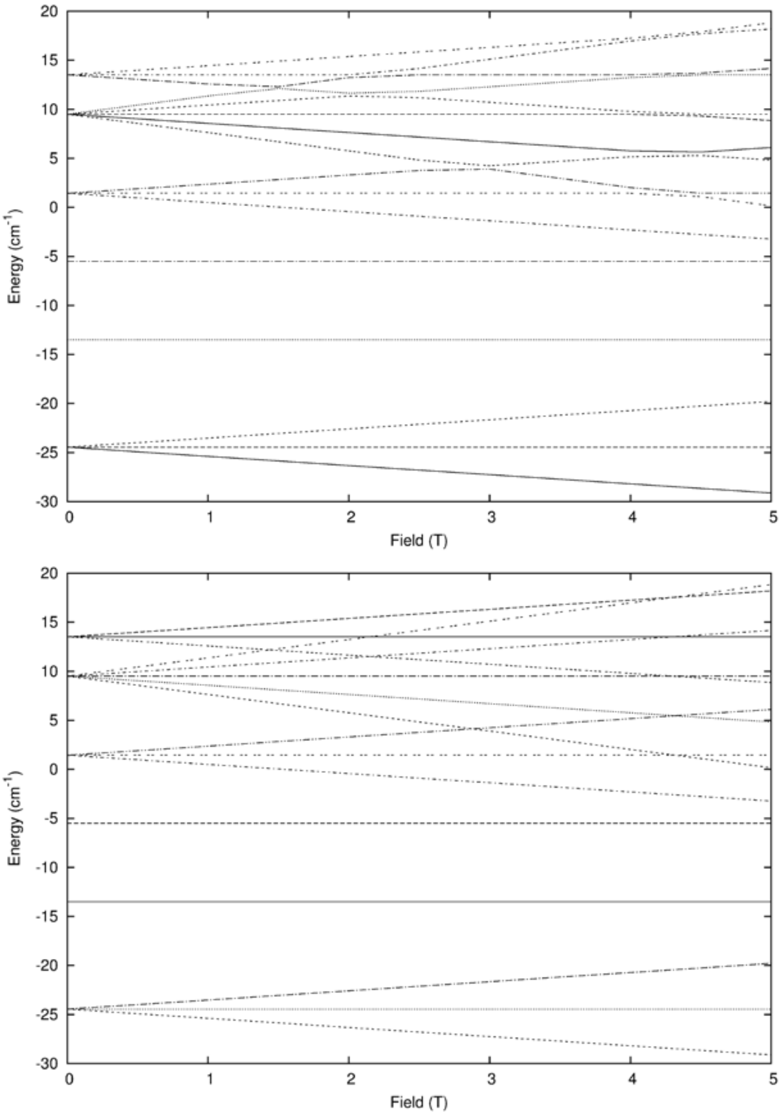

Figure 4.3.1 – Zeeman plots using a full calculation (top) and the approximation method (bottom)

*****Survey block*

To perform a parameter sweep, the “****Survey” block is utilized. The first line of this block specifies what the user wishes to survey. For example, if the first line is ‘Residual’ the output will be the residual error between the calculation and experiment against the parameters in the survey. Other options include ‘M(i,j)’, ‘S(i,j)’, ‘C(i,j)’ or ‘H(i,j)’, which represent the value of the magnetization, susceptibility, MCE or heat capcity respectively, for the ith field and the jth temperature. Following the first line, this block is internally delimited into sections which belong to the same variable, by “----”; this delimiter ***must be present*** even at the end of the final section as shown below. The start and end values for the parameter and the number of steps required are first specified, followed by the properties that they control. In the following example, the exchange coupling parameter is varied between -10 and 10 cm^{-1} in 20 steps and the isotropic g-factors of sites 1 and 4 are varied from 1.7 to 2.3 in 10 steps.

```
****Survey
Residual
-10.0 10.0  20
EX    1     2     4
----
1.7   2.3   10
GF    1     4
GF    4     4
----
```

Table 4.3.9 lists the syntax for different properties; note that the dummy integers (zeros) must be present.

Table 4.3.9 – ****Fit and ****Survey block syntax

Syntax	Comment
EX SiteA SiteB 1/2/3/4/5/6/7	Exchange coupling, third integer represents x, y, z, isotropic, antisymmetric x, antisymmetric y or antisymmetric z.
IN SiteA SiteB 1/2/3/4/5/6/7/8/9	Interaction tensor, third integer represents Jxx, Jxy, Jxz, Jyx, Jyy, Jyz, Jzx, Jzy or Jzz.
SO Site 1/2/3/4/5/6	Spin-orbit coupling, second integer is the order.
GF Site 1/2/3/4	G-factor, second integer represents x, y, z or isotropic.
CF Site Rank Order	Crystal field parameter.
RC Site 1/2/3	Reference frame rotation, second integer represents α, β or γ.
RE SiteA SiteB 1/2/3	Exchange frame rotation, third integer represents α, β or γ.
OR Site	Orbital reduction parameter.
LW Freq. 1/2/3/4	EPR linewidth, second integer selects corresponding frequency (0 applies to all frequencies), third integer represents x, y, z, or isotropic
VO Freq.	EPR pseudo-voigt parameter, second integer selects corresponding frequency, where 0 implies all frequencies.
MO Freq.	EPR mosacity, second integer selects corresponding frequency, where 0 implies all frequencies.
TI	Temperature Independent Paramagnetism.
DT	Debye temperature.
DA	Debye exponent.
ZJ	Mean-field intermolecular interaction.
IM	Monomeric impurity.
ES SiteA SiteB 1/2/3/4/5/6/7	Exchange strain, third integer represents x, y, z,

				isotropic, antisymmetric x, antisymmetric y or antisymmetric z.
IS	SiteA	SiteB	1/2/3/4/5/6/7/8/9	Interaction strain, third integer represents Jxx, Jxy, Jxz, Jyx, Jyy, Jyz, Jzx, Jzy or Jzz.
SS	Site	1/2/3/4/5/6		Spin-orbit coupling strain, second integer is the order.
GS	Site	1/2/3/4		G-factor strain, second integer represents x, y, z or isotropic.
CS	Site	Rank	Order	Crystal field strain.
OS	Site			Orbital reduction strain.

*****Fit block*

To fit experimental data, the "****Fit" block must be detailed. This block is very similar in syntax to the ****Survey block, however in place of the start, finish and number of steps, ***either*** the starting value for the parameter ***or*** the lower limit, starting value and upper limit is required. Before the beginning of the variable sub-blocks, the first line is either "Powell" or "Simplex", specifying the fitting algorithm to be used. The example below would fit four different isotropic exchange couplings between different pairs of spins, and the isotropic *g*-factor for sites 1 to 4, limited between 1.9 and 2.1, using the Simplex method.

Note that only the parameters tied to variables in the ****Fit block will be altered in the fitting procedure and all other parameters defined in the input file are fixed.

```
****Fit
Simplex
-2.0
ex 1 2 4
----
1.0
ex 1 3 4
ex 2 4 4
----
1.5
ex 1 4 4
ex 2 3 4
----
0.1
ex 3 4 4
----
1.9 2 2.1
gf 1 4
gf 2 4
gf 3 4
gf 4 4
----
```

*****Params block*

Finally, the “****Params” block is used to choose the operation mode and other calculation options. Table 4.3.10 gives the options available in this section.

Table 4.3.10 – ****Params block options

Parameter	Options/Syntax	Comments
Operation mode	OpMode STR1 STR2	Selection of operation mode, STR1 and STR2 are strings, see Table 4.3.10. ***Must be present***.
Magnetism approximation	Approx	Turns on the block diagonal approximation for isotropic systems. Default = Off.
Monomeric impurity	IMP N x	Adds a monomer impurity of spin S = N/2, with fraction x, i.e. x = 1 for one uncoupled spin. Default = Off.
Zero field splitting	ZFS I J K …	Alters the convention of B_0^2 such that it equals D. Any number of sites can be listed on the same line. Default = Off.
Cubic crystal field	Cubic I J K …	Forces cubic CFP ratios for B_4^4 and B_6^4 based on B_4^0 and B_6^0. Any number of sites can be listed on the same line. Default = Off.
Static magnetic field	StaticB |B| X Y Z StaticB |B| θ φ	Includes the presence of a static magnetic field of magnitude |B| Tesla, with vector (X,Y,Z) or polar coordinates (θ,φ) in degrees. Default = Off.
Rotate reference frame	Rotate N α β γ	Rotates the reference frame (CFPs and or g) for site N, through the Euler angles α, β and γ, given in degrees. Default = Off.
Rotate exchange frame	EXRotate N M α β γ	Rotates the exchange frame for the exchange defined between sites N and M, through the Euler angles α, β and γ, given in degrees. Default = Off.
Number of CPU cores	MaxCPU N	Sets the upper limit of CPU cores available, N is an integer. Default = “MaxCPU cores-1”.
Fitting algorithm display	NoPrint	Turns off the printing of fit progress to the terminal and intermediate results to disk. Default = Off.
Full wavefunction printing	FullWF	Prints the full wavefunction in the states.res file. Default = Off.
Save survey calculations	Save	Saves a file for each step of the survey calculation. Default = Off.
Disable operator equivalent factors	NoOEF	Disables the Operator Equivalent Factors such that CF input values are assumed to contain θ_k. Default = Off.
G-tensor multiplets	Mults N A B C D …	Gives the multiplicities of the multiplets for the calculations of pseudo-spin $\tilde{S} = \frac{1}{2}$ states. N

		gives the number of multiplets, followed by N integers giving the multiplicity. Default = Off.
Single crystal experiment	Single	Circumvents checking for the need to integrate magnetic properties – i.e. requested single field direction is allowed. Default = Off.
Percentage completion	Percent	Prints percentage completion for command line operation. Default = Off.
Residual type	Residual STR	Selects residual calculation method. STR is a string, see Table 4.3.13. Default = Off.
G-tensor direction residual	GDir STR	Selects which directions to include in the residual calculation for g-tensors (and directions). STR is a string of x, y, z or a combination thereof. Default = “GDir xyz”.
Fitting algorithm vigour	FitVigour X	Sets how vigourous the fitting algorithm starts, as a parameter percentage. Default = “FitVigour 10”.
Fitting algorithm limiting	FitLimit X	Sets how strongly the fitting algorithm enforces parameter limits. Limiting function is $e^{X\|\Delta\|}$, where Δ is difference between the fitting parameter and its limit. Default = “FitLimit 12”.
Fitting algorithm iteration limit	FitIter N	Sets an upper limit for the number of fit iterations. Default = no limit.
Fitting algorithm tolerance	FitTolerance X	Sets the tolerance threshold for completing the fitting algorithm. Default = “FitTolerance 1E-12”.
Disable uncertainties in fit parameters	NoUncertainties	Disables the calculation of uncertainties in the fitting variables. Default = On.
Orbital Reduction in Zeeman term	ORedOnlyZeeman	Restricts the application of the orbital reduction parameter to the orbital Zeeman term only. Default = Off.
High-precision output	HighPrec	Prints results to machine precision. Default = Off.

Table 4.3.11 – Operation modes

OpMode	Comments
Sim STR2	Simulation; STR2 is a string, see below and Table 4.3.11.
Fit STR2	Fit; STR2 is a string, see below and Table 4.3.11.
Sur STR2	Survey; STR2 is a string, see below and Table 4.3.11.
Coupling Report	Reports the block diagonal structure of the matrix
Matrix Elements	Prints Hamiltonian matrix

The second required string is composed of letters representing the calculations to be performed. For example, “MS” would represent Magnetization and Susceptibility, whilst “LSG” would represent energy Levels, Susceptibility and G-tensors. The possible letters are given in Table 4.3.12. Note that a Simulation involving L (energy levels) will result in the printing of the wavefunction in states.res, that G and D are mutually exclusive and that the letter codes may be in any order (i.e. LMSG ≡ MGLS etc.).

Table 4.3.12 – Operation mode STR2

STR2	Comments
L	Energy levels
M	Magnetization
S	Susceptibility
T	Susceptibility Tensor
G	G-tensors
D	G-tensors with directions
C	MCE
H	Heat capacity
E	EPR
Z	Zeeman

The number of directions used with the ZCW integration scheme is not a linear trend with ZCW level. Table 4.3.13 shows the number of directions for each ZCW level up to 20.

Table 4.3.13 – Number of directions in ZCW integration

ZCW	Number
0	21
1	34
2	55
3	89
4	144
5	233
6	377
7	610
8	987
9	1597
10	2584
11	4181
12	6765
13	10946
14	17711
15	28657
16	46368

17	75025
18	121393
19	196418
20	317811

The options for the residual types can be used to favour better fitting of particular regions of data.

Table 4.3.14 – Residual types

Residual type string	Comments
LowT	Low temperature bias
HighT	High temperature bias
LowB	Low field bias
HighB	High field bias
LowT/LowB	Low temperature and low field bias
LowT/HighB	Low temperature and high field bias
HighT/LowB	High temperature and low field bias
HighT/HighB	High temperature and high field bias
LowE	Low energy bias
HighE	High Energy bias

Data file specification

Experimental data files follow similar formats for all experimental types; they are plain text files with extensions _sus.exp, _mag.exp, _mce.exp, etc. The general format is that the independent variable (field, temperature, etc.) is given in the first column, followed by columns with the corresponding experimental data where each column is a different data set (different temperature, field, frequency, etc.). For all experimental data files, there need not be a data point for every given independent variable; that is, for a particular data set some points may be missing, in which case any symbol of . or ! or ? or # or // or * may be given. In this way, the values of the independent variable need not be consistent between data sets, but the data file must have a fixed number of rows for each column. Note that there should be no blank lines at the end of the file.

The specific layout for each experimental data type are given below.

Susceptibility (_sus.exp):

The first column represents the temperature in K and the subsequent columns represent the experimental data ($\chi_M T$) in cm^3 mol^{-1} K for the different fields as defined in the .input file, for example 0.01, 0.1 and 1 T respectively.

```
T1    B1    B2    B3
T2    B1    B2    B3
T3    B1    B2    B3
etc.
```

Magnetization (_mag.exp):

The first column represents the magnetic field in T and the subsequent columns represent the experimental data (M) in Bohr Magnetons per mole ($N_A\mu_B$) for the different temperatures as defined in the .input file.

```
B1    T1    T2    T3
B2    T1    T2    T3
B3    T1    T2    T3
etc.
```

Magnetic Susceptibility Tensor (_tensor.exp):

The first column represents the temperature in K and the subsequent columns represent the six unique elements of the $\chi_M T$ tensor (with the order $\chi_{xxM}T$, $\chi_{xyM}T$, $\chi_{xzM}T$, $\chi_{yyM}T$, $\chi_{yzM}T$, $\chi_{zzM}T$) in cm^3 mol^{-1} K for the different fields as defined in the .input file.

```
T1    B1,xx B1,xy B1,xz B1,yy B1,yz B1,zz B2,xx B2,xy B2,xz B2,yy B2,yz B2,zz
T2    B1,xx B1,xy B1,xz B1,yy B1,yz B1,zz B2,xx B2,xy B2,xz B2,yy B2,yz B2,zz
T2    B1,xx B1,xy B1,xz B1,yy B1,yz B1,zz B2,xx B2,xy B2,xz B2,yy B2,yz B2,zz
etc.
```

Magneto-caloric Effect (_mce.exp):

The first column represents the temperature points in K and the subsequent columns represent the experimental data ($-\Delta S$) in J kg^{-1} K^{-1} for the different magnetic fields. Note that the appropriate molecular mass must be defined in the ****Params* block.

```
T1    B1    B2    B3
T2    B1    B2    B3
T3    B1    B2    B3
etc.
```

Heat Capacity (_heat.exp):

The first column represents the temperature points in K and the subsequent columns represent the experimental data (C) in units of R (J mol^{-1} K^{-1}) for the different magnetic fields.

```
T1    B1    B2    B3
T2    B1    B2    B3
T3    B1    B2    B3
etc.
```

Electron Paramagnetic Resonance (_epr.exp):

The first column represents the magnetic field points in T and the subsequent columns represent the experimental data (either integrated absorbance, absorbance, first derivative or second derivative) for the different frequencies and temperatures. The data should be normalized to the magnitude of the largest peak (positive or negative), at the first temperature in the input file. Note that the temperature is the inner loop and varies first, followed by the frequency.

```
B1    F1,T1 F1,T2 F1,T3 F2,T1 F2,T2 F2,T3
B2    F1,T1 F1,T2 F1,T3 F2,T1 F2,T2 F2,T3
B3    F1,T1 F1,T2 F1,T3 F2,T1 F2,T2 F2,T3
etc.
```

Energy levels (_levels.exp):

The format for this file is one floating point value per line, for each energy level, given in wavenumbers.

```
E1
E2
E3
E4
etc.
```

G-tensor (_G.exp)

This file is used to define the experimental g-tensors used for the fitting and survey modes. The file consists of lines with three ***or*** twelve values, defining either g_x, g_y and g_z ***or*** g_x, g_y, g_z, $D^i_{g_x}$, $D^j_{g_x}, D^k_{g_x}, D^i_{g_y}, D^j_{g_y}, D^k_{g_y}, D^i_{g_z}, D^j_{g_z}, D^k_{g_z}$ for each Kramers doublet, where $D^i_{g_\alpha}, D^j_{g_\alpha}, D^k_{g_\alpha}$ is the unit vector denoting the direction of g_α. Each line represents the diagonalized g-tensor for a pseudo-spin 1/2 Kramers doublet. Therefore, the number of g-tensors must be less than or equal to half the total dimension of the problem.

```
gx1   gy1   gz1
gx2   gy2   gz2
gx3   gy3   gz3
etc.
```

or

```
gx1   gy1   gz1    Digx1  Djgx1  Dkgx1  Digy1  Djgy1  Dkgy1  Digz1  Djgz1  Dkgz1
gx2   gy2   gz2    Digx2  Djgx2  Dkgx2  Digy2  Djgy2  Dkgy2  Digz2  Djgz2  Dkgz2
gx3   gy3   gz3    Digx3  Djgx3  Dkgx3  Digy3  Djgy3  Dkgy3  Digz3  Djgz3  Dkgz3
etc.
```

4.4 Output files and interpretation

PHI outputs information regarding the operation of the program and the type of calculations it is performing to stdout (shell, command prompt or terminal). This is redirected to the GUI output panel, however when running *PHI* without a GUI, this can be directed to a specified output file by appending, for example, “> test-job.out” to the execution command, so that it would read on Linux “./phi_vx.x_linux64.x test-job > test-job.out”. *PHI* writes all calculated data to files in the working directory of the job, in the files described below. Note that the naming of the files is identical to that of the .exp input data files – the job name is appended with an underscore to the following output files, for example “test-job_mag.res”.

sus.res, tensor.res, mag.res, mce.res, heat.res, epr.res, levels.res and G.res specification

Data is written to this file in exactly the same format as the input .exp files.

zeeman.res specification

This file contains the results from a calculation of a Zeeman plot. The file consists of $dim + 1$ columns, where dim is the dimension of the total Hilbert space of the system. The first column contains the magnetic field strength (B) in Tesla, followed by the corresponding energy for each state in the system in wavenumbers.

survey.res specification

This file contains a number of columns, one for each operator defined in the ‘****Survey’ block and one more, the final column, which represents the residual for the parameter set defined by the row, noting that the columns are ordered as the variables in the ‘****Survey’ block.

states.res specification

This file is produced when a simulation of the energy levels is requested and contains information regarding the wavefunction and energy levels and transition probabilities, J-mixing and g-tensors, if applicable. In the full calculation case, the wavefunction is printed in a matrix type manner, with row and column headers. The first column contains the row headers which are the basis elements in which the Hamiltonian was constructed, i.e. the single ion states. The subsequent columns are the different eigenstates of the system, with the column headers displaying the energies in wavenumbers. The columns show the expansion coefficients for the basis states that comprise the given eigenstate. Unless “FullWF” is selected, coefficients below 1×10^{-10} are not printed. In the case of wavefunctions with imaginary components, two matrices are printed; the top one being the real part of the coefficients and the bottom one being the imaginary components. Below this are shown the percentage contribution of each basis state to the wavefunction. For anisotropic systems, the transition probabilities between the states are printed – note that this matrix is symmetric. For single lanthanide ions calculated under the simple input method, the wavefunction is also transformed into the $\left|J_i, m_{J_i}\right\rangle$ basis and is printed in the same manner as that for the regular wavefunction. If the g-tensor calculation is appropriate, the diagonal g-tensors are printed along with their directions in the internal coordinate system.

In the approximation mode, a list of the intermediate and final spin states along with their energies are provided. Additionally, the effective g-values for the coupled spin states and the spin projection coefficients for each metal site are given.

4.5 Use of the GUI

Figure 4.5.1 shows a screenshot of the GUI in operation under Windows 7. The interface is divided into three sections. The main left pane is for *PHI* input, the upper right pane is for displaying results and the lower right pane shows the *PHI* output including error messages. The settings window allows the user to change various display options, and are saved between sessions, including the window size and position, and last working directory.

When simulating EPR spectra, in addition to the calculated EPR data, the orientation-dependent Zeeman spectra are shown along with the most intense EPR transition for each frequency. The direction can be chosen using the slider below the plot.

The ‘Copy .res to .exp’ button in the Tools menu provides the user the option to automatically copy the calculated data to experimental files, overwriting any existing experimental data (be careful!). This facilitates comparison between different parameter sets or for testing how sensitive a parameterisation is to specific features.

The ‘Save plots’ button in the Tools menu saves the active plots as .pdfs for editing or publication in vector format.

```
****spin
3
****crystal field
1 2 0 -0.2
1 2 2 0.09
****epr
fepr 9.4
tepr 5 7.5 10
sweep 0 0.7 800
lw 1.5
field powder 7
****fit
simplex
-0.15
cf 1 2 0
----
0.12
cf 1 2 2
----
1.8
lw 0 4
----
****params
cpmode fit w
sfs 1
****end
```

```
==========================================
Iteration:          9
------------------------------------------
-0.179166666666667
CF   1  2  0
==========================================
0.107333333333332
CF   1  2  2
==========================================
2.030000000000002
LW   0  4
------------------------------------------
Residual: 79.622697540281421
==========================================
```

Figure 4.5.1 – Screenshot of *PHI* in operation on Windows 7

4.6 Examples

Cu(OAc)$_2$

The classic Cu(II)$_2$(OAc)$_4$ dimer, originally investigated by Bleaney and Bowers[47] and subsequently by Gerloch *et al.*,[48] shows a strong decrease in the $\chi_M T$ vs. T data with a reduction in temperature. Such behaviour originates from anti-ferromagnetic superexchange between the Cu(II) ions, leading to an $S = 0$ ground state. To investigate the magnitude of the superexchange interaction, a fit of the $\chi_M T$ vs. T data to a single-J isotropic HDVV spin Hamiltonian with a variable g-factor in the Zeeman Hamiltonian, was performed. The entire input file required to perform this calculation with *PHI* is presented to highlight the simplicity of such operations, Figure 4.6.1 (inset). This analysis found a very good fit to the experimental data, Figure 4.6.1, with a coupling constant of $J = -144.6\ \text{cm}^{-1}$ and $g = 2.12$.

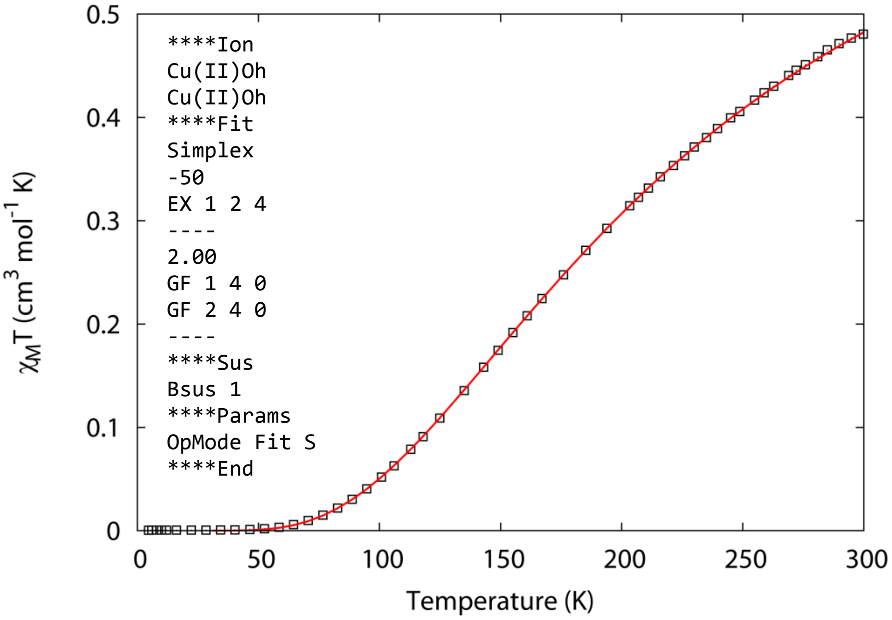

```
****Ion
Cu(II)Oh
Cu(II)Oh
****Fit
Simplex
-50
EX 1 2 4
----
2.00
GF 1 4 0
GF 2 4 0
----
****Sus
Bsus 1
****Params
OpMode Fit S
****End
```

Figure 4.6.1 – Magnetic susceptibility of the $Cu(II)_2(OAc)_4$ dimer in a field of 1 T, the solid line is a fit to the data using the parameters in the text. Inset: Entire *PHI* input file required to perform the calculation.

Modelling high-spin octahedral Co(II) ions

Summarising section 2.2, the *PHI* Hamiltonian is given by Equation 4.6.1.

$$\hat{H} = \sum_{i=1}^{N}\sum_{j=1}^{2S_i} \lambda_{j_i} \left(\sigma_i \vec{\hat{L}}_i \cdot \vec{\hat{S}}_i\right)^j + -2\sum_{i<j}^{i,j\in N} \vec{\hat{S}}_i \cdot \overline{\overline{J_{ij}}} \cdot \vec{\hat{S}}_j + \sum_{i=1}^{N}\sum_{k=2,4,6}\sum_{q=-k}^{k} \sigma_i{}^k B_{k\,i}^{q} \theta_k \hat{O}_{k\,i}^{q}$$

$$+ \mu_B \sum_{i=1}^{N} \left(\sigma_i \vec{\hat{L}}_i \cdot \overline{\overline{I}} + \vec{\hat{S}}_i \cdot \overline{\overline{g_i}}\right) \cdot \vec{B}$$

(4.6.1)

By default all $L_i = 0$, $\lambda_{j_i} = 0$, $\sigma_i = 1$, $\overline{\overline{J_{ij}}} = \begin{bmatrix} 0 & 0 & 0 \\ 0 & 0 & 0 \\ 0 & 0 & 0 \end{bmatrix}$., $B_{k\,i}^{q}\theta_k = 0$ and $\overline{\overline{g_i}} = \begin{bmatrix} 2 & 0 & 0 \\ 0 & 2 & 0 \\ 0 & 0 & 2 \end{bmatrix}$.

To treat high-spin octahedral Co(II), we will use the T≡P equivalence (isomorphism) method,[19] which uses a fictional orbital angular momentum of $L = 1$ to model the triplet orbital state. In this approach, we set $S_1 = \frac{3}{2}$, $L_1 = 1$, $\lambda_{1_1} \approx -171.5\ cm^{-1}$ and $\sigma_1 = -\frac{3}{2}$, leaving other parameters as default. This can be done as follows:

```
****Spin
3
****Orbit
2
****SOCoupling
1 -171.5
****OReduction
1 -1.5
****Paramps
OpMode Sim L
****End
```

Or equivalently:

```
****Ion
Co(II)Oh(w)
****Params
OpMode Sim L
****End
```

The latter approach using the *****Ion* block engages (only) the constants given in Table 4.3.1. In either case, the parameters are modified in the same way, by changing the values with the blocks. For example:

```
****Spin
3
****Orbit
2
****SOCoupling
1 -160
****OReduction
1 -1.0
****Params
OpMode Sim L
****End
```

Or equivalently:

```
****Ion
Co(II)Oh(w)
****SOCoupling
1 -160
****OReduction
1 -1.0
****Params
OpMode Sim L
****End
```

In the latter case, the use of the *****SOCoupling* and *****OReduction* blocks overrides the defaults switched on by the *****Ion* block.

In order to employ an orbital reduction factor with a high-spin octahedral Co(II) site, we probably want to do something like Equation 4.6.2 (i.e. this is what would be written in a manuscript).

$$\hat{H}_{ZEE} = \mu_B \sum_{i=1}^{N} \left(-\frac{3}{2}\kappa_i \vec{\hat{L}}_i \cdot \bar{\bar{I}} + \vec{\hat{S}}_i \cdot \bar{\bar{g}}_i \right) \cdot \vec{B} \tag{4.6.2}$$

However in *PHI* the Hamiltonian is fixed as Equation 4.6.3.

$$\hat{H}_{ZEE} = \mu_B \sum_{i=1}^{N} \left(\sigma_i \vec{\hat{L}}_i \cdot \bar{\bar{I}} + \vec{\hat{S}}_i \cdot \bar{\bar{g}}_i \right) \cdot \vec{B} \tag{4.6.3}$$

Therefore, we must use $\sigma_i = -\frac{3}{2}\kappa_i$. Then, if $0 < \kappa_i \leq 1$ we have $0 > \sigma_i \geq -\frac{3}{2}$, corresponding to the limits of full orbital reduction and no orbital reduction, respectively. This follows the notation of Lloret *et. al.* (section 3.1.1.1 of reference [19]), where the origin of $\kappa \leq 1$ and changes in the $-\frac{3}{2}$ factor (referred to as A) are described, where both factors are combined together to avoid over-parameterization (*i.e.* a rise in one is compensated by a fall in the other, so they cannot be fitted independently to find a unique solution).

Note that *PHI* must be fully general and permit application to true orbital states, therefore σ_i can also be the real orbital reduction factor (i.e. $\sigma_i = \kappa_i$) and take the range $0 < \sigma_i \leq 1$ in other cases.

Back to high-spin octahedral Co(II); in this case we implicitly assume the geometry is perfectly octahedral, however this is rarely true. Therefore, we can model the *distortions from octahedral symmetry* with effective crystal field parameters acting on the fictional orbital angular momentum, representing a splitting of the t_{2g} orbitals. For example, high-spin axially distorted octahedral Co(II), could be described with Equation 4.6.4, and modelled in PHI as below.

$$\hat{H} = \sigma\lambda\vec{\hat{L}} \cdot \vec{\hat{S}} + \sigma^2 v\left(3\hat{L}_z{}^2 - \hat{L}^2\right) + \mu_B\left(\sigma\vec{\hat{L}}_i \cdot \bar{\bar{I}} + \vec{\hat{S}}_i \cdot g\bar{\bar{I}}\right) \cdot \vec{B} \tag{4.6.4}$$

where σ is the combined orbital reduction parameter ($\sigma = -\frac{3}{2}\kappa$)

λ is the SO coupling parameter

v is the axial distortion parameter

g is the isotropic spin g-value

```
****Spin
3
****Orbit
2
****SOCoupling
1 λ
****OReduction
1 σ
****CrystalField
1 2 0 v
****GFactor
1 g
****Params
OpMode Sim L
****End
```

Or equivalently:

```
****Ion
Co(II)Oh(w)
****SOCoupling
1 λ
****OReduction
1 σ
****CrystalField
1 2 0 v
****GFactor
1 g
****Params
OpMode Sim L
****End
```

4.7 Testing

The “Coupling Report” Operation Mode is provided to inform the user of the block diagonal structure of the HDVV Hamiltonian matrix in a coupled total spin basis, without performing any demanding calculations. It is useful to check to see the requirements of large problems and determine whether it can be solved on the available hardware.

5. Bugs and Feedback

The development of *PHI* is an on-going process, which the author hopes will continue with the advent of new technologies and/or interfaces, which may enhance the computational power available to the user. The author welcomes any bug reports, feature requests, comments, suggestions or queries about the code. Please address all correspondence to nfchilton@gmail.com.

Please keep in mind that the code is continually under development and bugs may still be present. Updated source code and binaries are uploaded to www.nfchilton.com/phi regularly.

6. References

1 N. Karayianis, *J. Chem. Phys.*, 1970, **53**, 2460–2469.

2 N. F. Chilton, R. P. Anderson, L. D. Turner, A. Soncini and K. S. Murray, *J. Comput. Chem.*, 2013, **34**, 1164–1175.

3 R. J. Elliott and M. F. Thorpe, *J. Appl. Phys.*, 1968, **39**, 802–807.

4 O. Kahn, *Mol. Phys.*, 1975, **29**, 1039–1051.

5 J. J. Borrás-Almenar, J. M. Clemente-Juan, E. Coronado, A. V. Palii and B. S. Tsukerblat, *Chem. Phys.*, 2001, **274**, 131–144.

6 W. P. Wolf, *J. Phys. Colloq.*, 1971, **32**, C1-26-C1-33.

7 A. Palii, B. Tsukerblat, J. M. Clemente-Juan and E. Coronado, *Int. Rev. Phys. Chem.*, 2010, **29**, 135–230.

8 M. E. Lines, *J. Chem. Phys.*, 1971, **55**, 2977–2984.

9 M. Hutchings, in *Solid State Physics*, Elsevier, Amsterdam, 1964, vol. 16, pp. 227–273.

10 C. E. Schäffer and C. K. Jørgensen, *Mol. Phys.*, 1965, **9**, 401–412.

11 W. Urland, *Chem. Phys.*, 1976, **14**, 393–401.

12 D. J. Newman and B. Ng, *Rep. Prog. Phys.*, 1989, **52**, 699–762.

13 J. Mulak and Z. Gajek, *The Effective Crystal Field Potential*, Elsevier, 2000.

14 C. Rudowicz, *J. Phys. C Solid State Phys.*, 1985, **18**, 1415–1430.

15 B. Bleaney and K. W. H. Stevens, *Rep. Prog. Phys.*, 1953, **16**, 108–159.

16 K. W. H. Stevens, *Proc. Phys. Soc. Sect. A*, 1952, **65**, 209–215.

17 A. Abragam and B. Bleaney, *Electron Paramagnetic Resonance of Transition Ions*, Oxford University Press, 1970.

18 C. Gorller-Walrand and K. Binnemans, in *Handbook on the Physics and Chemistry of Rare Earths*, Elsevier, 1996, vol. 23.

19 F. Lloret, M. Julve, J. Cano, R. Ruiz-García and E. Pardo, *Inorganica Chim. Acta*, 2008, **361**, 3432–3445.

20 R. Boča, *Theoretical Foundations of Molecular Magnetism*, Elsevier, 1999.

21 M. Evangelisti and E. K. Brechin, *Dalton Trans.*, 2010, **39**, 4672.

22 M. Evangelisti, F. Luis, L. J. de Jongh and M. Affronte, *J. Mater. Chem.*, 2006, **16**, 2534.

23 J. J. Borrás-Almenar, J. M. Clemente-Juan, E. Coronado and B. S. Tsukerblat, *J. Comput. Chem.*, 2001, **22**, 985–991.

24 J. J. Sakurai and S. F. Tuan, *Modern quantum mechanics*, Addison-Wesley Longman, 2010.

25 J. J. Borrás-Almenar, J. M. Clemente-Juan, E. Coronado and B. S. Tsukerblat, *Inorg. Chem.*, 1999, **38**, 6081–6088.

26 D. Gatteschi and L. Pardi, *Gazzetta Chim. Ital.*, 1993, **123**, 231–240.

27 B. W. Shore and D. H. Menzel, *Principles of atomic spectra*, Wiley, 1967.

28 A. Bencini and D. Gatteschi, *EPR of Exchange Coupled Systems*, Springer-Verlag, 2012.

29 M. Eden and M. H. Levitt, *J. Magn. Reson.*, 1998, **132**, 220–239.

30 M. Gerloch and R. F. McMeeking, *J. Chem. Soc. Dalton Trans.*, 1975, 2443–2451.

31 H. Bolvin, *ChemPhysChem*, 2006, **7**, 1575–1589.

32 J. Mulak and M. Mulak, *Phys. Status Solidi B*, 2006, **243**, 2796–2810.

33 G. R. Hanson, K. E. Gates, C. J. Noble, M. Griffin, A. Mitchell and S. Benson, *J. Inorg. Biochem.*, 2004, **98**, 903–916.

34 S. Stoll and A. Schweiger, *J. Magn. Reson.*, 2006, **178**, 42–55.

35 S. D. Bruce, J. Higinbotham, I. Marshall and P. H. Beswick, *J. Magn. Reson.*, 2000, **142**, 57–63.

36 H. Husein Mor, H. Weihe and J. Bendix, *J. Magn. Reson.*, 2010, **207**, 283–286.

37 G. van Veen, *J. Magn. Reson. 1969*, 1978, **30**, 91–109.

38 R. Aasa and tore Vänngård, *J. Magn. Reson. 1969*, 1975, **19**, 308–315.

39 S. K. Klitgaard, F. Galsbøl and H. Weihe, *Spectrochim. Acta. A. Mol. Biomol. Spectrosc.*, 2006, **63**, 836–839.

40 R. P. Feynman, *Phys. Rev.*, 1939, **56**, 340–343.

41 G. A. F. Seber and C. J. Wild, *Nonlinear regression*, Wiley, New York, 1989.

42 M. J. D. Powell, *Comput. J.*, 1964, **7**, 155–162.

43 J. A. Nelder and R. Mead, *Comput. J.*, 1965, **7**, 308–313.

44 W. H. Press, S. A. Teukolsky, W. T. Vetterling and B. P. Flannery, *Numerical Recipes in Fortran 90: The Art of Parallel Scientific Computing*, Cambridge University Press, 2nd edn., 1996.

45 P. D. Stevenson, *Comput. Phys. Commun.*, 2002, **147**, 853–858.

46 E. Eichhammer, Qt Plotting Widget QCustomPlot - Introduction, http://www.qcustomplot.com/, (accessed October 6, 2016).

47 B. Bleaney and K. D. Bowers, *Proc. R. Soc. Math. Phys. Eng. Sci.*, 1952, **214**, 451–465.

48 M. Gerloch and J. H. Harding, *Proc. R. Soc. Math. Phys. Eng. Sci.*, 1978, **360**, 211–227.